

Cite this: *Chem. Sci.*, 2024, **15**, 7824

All publication charges for this article have been paid for by the Royal Society of Chemistry

Received 7th February 2024  
Accepted 27th April 2024

DOI: 10.1039/d4sc00933a

rsc.li/chemical-science

# Supramolecular chemistry of liquid–liquid extraction

Sourav Pramanik, Abu S. M. Islam, Iti Ghosh and Pradyut Ghosh\*

Liquid–Liquid Extraction (LLE) is a venerable and widely used method for the separation of a targeted solute between two immiscible liquids. In recent years, this method has gained popularity in the supramolecular chemistry community due to the development of various types of synthetic receptors that effectively and selectively bind specific guests in an aqueous medium through different supramolecular interactions. This has eventually led to the development of state-of-the-art extraction technologies for the removal and purification of anions, cations, ion pairs, and small molecules from one liquid phase to another liquid phase, which is an industrially viable method. The focus of this perspective is to furnish a vivid picture of the current understanding of supramolecular interaction-based LLE chemistry. This will not only help to improve separation technology in the chemical, mining, nuclear waste treatment, and medicinal chemistry sectors but is also useful to address the purity issue of the extractable species, which is otherwise difficult. Thus, up-to-date knowledge on this subject will eventually provide opportunities to develop large-scale waste remediation processes and metallurgy applications that can address important real-life problems.

## 1. Introduction

Supramolecular chemistry is a branch of chemistry that focuses on the study of the design of molecular assemblies with smaller building units held together by non-covalent interactions.<sup>1</sup> These interactions include hydrogen bonding,  $\pi$ – $\pi$  stacking,

van der Waals forces, and other weak forces that mainly play a pivotal role in the assembly of molecules.<sup>2</sup> The term “supramolecular” emphasizes the scale of these structures, which is beyond the individual molecular level. Over the past few decades, supramolecular chemistry has held significance across diverse fields, including biology, medicine, materials science,

School of Chemical Sciences, Indian Association for the Cultivation of Science, Kolkata 700032, India. E-mail: icpg@iacs.res.in



Sourav Pramanik

Sourav Pramanik received his Bachelor's and Master's degrees in chemistry from Vidyasagar University, Midnapore, West Bengal. Thereafter, he joined the Indian Association for the Cultivation of Science as a Research Scholar in 2020 under the supervision of Prof. Pradyut Ghosh. He is currently working on anion chemistry, in particular, anion recognition and separation following various supramolecular interactions.



Abu S. M. Islam

Dr Abu S. M. Islam received his M.Sc. in inorganic chemistry from the Department of Chemistry, West Bengal State University, India. Later he obtained his PhD from Jadavpur University, under the supervision of Prof. Mahammad Ali in 2019. During his PhD, he worked on detection and bio-imaging for small biomolecules like nitric oxide (NO), HSNO (S-nitrosothiol), and thiols ( $S^{2-}/SH^-$ ). Currently, he is a postdoctoral fellow at the

Indian Association for the Cultivation of Science under the supervision of Prof. Pradyut Ghosh. His research interests include designing and executing chemical reactions for chalcogen bond based receptors for anion recognition as well as extraction.

and the separation and purification processes essential for environmental remediation.<sup>1,3</sup>

In the realm of purification techniques, liquid–liquid extraction (LLE) stands out as a conspicuous application of supramolecular chemistry, associated with the separation of hazardous substances from the environment and the extraction of valuable metals from ores. LLE, commonly known as solvent extraction, is a separation technique that entails transferring a solute from one solvent (diluent), typically water, to an immiscible organic solvent (extractant). Such extraction is a widely employed technique in chemical labs and industry for the isolation and purification of desired compounds from mixtures.

The significance of supramolecular chemistry in LLE lies in its ability to tailor non-covalent interactions to achieve selective and efficient extraction processes. In this dynamic field, researchers explore the development of supramolecular host–guest systems, where host molecules encapsulate guests through manipulating non-covalent interactions. These host–guest interactions can be exploited in LLE processes to enhance the separation of target compounds based on size, shape, or chemical properties.<sup>4</sup> Furthermore, the decomplexation or back-extraction of the extracted species could offer a reusable receptor. Additionally, supramolecular assemblies, by forming micelles and vesicles,<sup>5,6</sup> can also be utilized to encapsulate and transport specific molecules through liquid phases, contributing to the efficiency of extraction processes. From the industrial aspect, solvent extraction signifies the viability of this easily accessible LLE technique in terms of lower energy consumption as well as high production capacity.<sup>7,8</sup> Besides, in the metallurgy section, highly precious metals like gold (Au) and platinum (Pt) can be recovered from their metalate anions using solvent extraction.<sup>9</sup>

This extraction method has made significant strides in separation and purification during the past few decades, although alternative approaches based on solid–liquid extraction, selective precipitation, and crystallization are also important.<sup>4,10,11</sup> Many research groups have reviewed the field with a focus on supramolecular interactions but these are in specific areas including (i) anion extraction by both SLE (Solid–Liquid Extraction) and LLE methods;<sup>4</sup> (ii) extraction of ion pairs;<sup>12</sup> and (iii) supramolecular systems along with macrocycle-based extractants for their industrial and environmental applications.<sup>12–16</sup> However, complete coverage of LLE based on supramolecular interactions has not been discussed in other reviews published on a similar topic.

In this perspective, we will highlight the up-to-date (2023) efforts which have been made by researchers for the progress of host molecules capable of recognizing as well as extracting inorganic guests from the aqueous phase employing LLE. Particularly, the emphasis of this review will focus on the non-covalent supramolecular interactions used for the LLE process that include LLE of halides, oxo-anions, alkali metals and ion-pairs. Finally, we will discuss the problems and promises associated with the structural variety of the hosts influencing the extraction behaviour.

## 2. Principles of supramolecular LLE

Parallel to the simple extraction method, the fundamental principles underlying supramolecular LLE involve concepts such as the distribution coefficient and phase equilibrium.

From a supramolecular aspect, after agitating two solvents, some fraction of the solute or guest molecule (G) from the aqueous phase is shifted to the organic phase by forming the



Iti Ghosh

*Iti Ghosh completed her B.Sc. in chemistry from Bethune College under the University of Calcutta. In 2022, she obtained her M.Sc. degree in chemistry from the Indian Association for the Cultivation of Science and in the same year she started her research career under the guidance of Prof. Pradyut Ghosh, working on anion recognition and separation by halogen and chalcogen bond-based receptors.*



Pradyut Ghosh

*Pradyut studied at the Indian Institute of Technology Kanpur for a PhD with Parimal K. Bharadwaj and did his first postdoctoral work in the US at Texas A&M University with Richard M. Crooks during 1998–2000. He was an Alexander von Humboldt Fellow at the University of Bonn and Freie Universität Berlin in Fritz Vögtle's and Christoph Schalley's groups. Upon his return to India, he joined CSMCRI, Bhavnagar*

*and in 2007 he moved to the Indian Association for the Cultivation of Science (IACS), Kolkata as an Associate Professor. In 2011 he was promoted to Professor of Chemistry and he was Head, Department of Inorganic Chemistry (2012–2015), Associate Dean (2015–2018) and Chair, School of Chemical Sciences (2018–2021) at IACS. Pradyut's present research interests are recognition, extraction and chemical sensing of ions of environmental and biological relevance, catalysis and interlocked molecules.*





Fig. 1 (a) Schematic illustration of the liquid-liquid extraction process. (b) Conceptual sketch of the Hofmeister series.

host-guest complex (HG) (Fig. 1). Such shifting of the guest is driven by host-guest non-covalent interactions, for instance, hydrogen bonding,  $\pi$ -interactions, hydrophobic interactions, *etc.*<sup>17–22</sup> Transfer of the guest by the host molecule (H) is achieved at the interface of two solvents by the following equilibrium:



where  $[\text{G}]_{\text{aq}}$  and  $[\text{H}]_{\text{org}}$  denote the concentration of the guest and host present in the aqueous and organic phases respectively and in general  $[\text{H}_n\text{G}_n]_{\text{org}}$  simply represents the extracted concentration of the guest in the organic phase. Thus, the guest molecule distribution between the aqueous and organic phases signifies the extraction ability of the host or receptor molecules. Eventually, the extraction ability is quantified through both the extraction efficiency ( $E$ ) and distribution ratio ( $D$ ), where the extraction efficiency ( $E$ ) can be defined as the concentration of guest extracted to the organic phase  $[\text{G}]_{\text{org}}$  divided by the total concentration of guests before extraction  $[\text{G}]_{\text{T}}$  (eqn (2)). In addition, a 'distribution ratio' ( $D$ ) is the ratio of the post-extraction concentration of the guest present in organic  $[\text{G}]_{\text{org}}$  and aqueous phases  $[\text{G}]_{\text{aq}}$  respectively (eqn (3)).

$$E = [\text{G}]_{\text{org}}/[\text{G}]_{\text{T}} \quad (2)$$

$$D = [\text{G}]_{\text{org}}/[\text{G}]_{\text{aq}} \quad (3)$$

Furthermore, assuming the interactions like hydrolysis and other complex formations with the host molecules are

negligible, from eqn (1) the extraction equilibrium constant ( $K_{\text{ex}}$ ) can also be evaluated by:

$$K_{\text{ex}} = [\text{H}_n\text{G}_n]_{\text{org}}/([\text{G}]_{\text{aq}}^n \times [\text{H}]_{\text{org}}^n) \quad (4)$$

and eqn (4) can be re-written as

$$\log(D) = \log(K_{\text{ex}}) + n \log[\text{H}]_{\text{org}} \quad (5)$$

This equation (eqn (5)) is a useful guide for interpreting the stoichiometry for host-guest complexation during the extraction. Importantly, to achieve efficient separation, phase equilibrium plays a crucial role, where the rate of transfer of guest (G) between the two phases becomes constant, indicating that the distribution of the G between the phases has reached a balance. Hence, at equilibrium, the chemical potential of the G is the same in both phases. This equilibrium is driven by the association and dissociation kinetics of the host-guest complexes. Furthermore, during host-guest complexation, counterions have to be taken into account in the extraction process for the distribution of guests in the two immiscible aqueous and organic phases. In the LLE process, the counterions can compete with the guests for binding to the host, thereby affecting the distribution ratio and complicating the extraction process. Moreover, to maintain the electrical neutrality of the solution, the host-guest complex must be accompanied by the counterions into the organic phase during extraction. Hence, the counterions' affinity to the organic solvent impacts on the distribution ratio.<sup>23,24</sup> Alongside, the hydrophobic ions are surface active and adsorb at the interface of two immiscible solution phases.<sup>25</sup> Additionally, these ions exhibit a preference for partitioning into the organic phase due to their greater solubility in the organic phase compared to water. Consequently, this helps to maintain charge neutrality in the solution, facilitating the transfer of guests into the organic phase. Moreover, it also reduces the interference with the guests on extraction into the aqueous phase, leading to an enhancement in the selectivity and efficiency of the extraction process.

Supramolecular LLE relies on the above principles which are shaped by the specificities of host-guest interactions. Such interactions, governed by the design of the supramolecular hosts, dictate the selectivity and efficiency of the extraction process in these systems.

### 3. Supramolecular interactions in LLE

Hydrogen bonding is a common supramolecular interaction that involves the attraction between a hydrogen atom covalently bonded to an electronegative atom and a Lewis base having a lone pair of electrons. In this regard, amino (NH) and hydroxyl (OH) groups are widely employed as hydrogen bond donors.<sup>4</sup> Moreover, the polarised CH bonds of heteroaromatic rings such as in imidazoles and triazoles can also offer excellent hydrogen bonding with the guest of interest.<sup>26</sup> To date, the majority of supramolecular receptors comprising this non-covalent interaction have been extensively utilized for LLE.

In addition, LLE may also be assisted by a Lewis base interaction with an electrophilic region or 'σ-hole' associated with halogen or chalcogen atoms in a molecule.<sup>27</sup> In the last decade, these σ-hole based non-covalent interactions have attracted attention in supramolecular chemistry due to their beneficial characteristics such as high directionality and hydrophobicity compared to hydrogen bonding. Nonetheless, these interactions are scarcely utilized for the LLE process.

In supramolecular chemistry, aromatic π-systems are considered crucial building units due to their ability to non-covalently interact with several functional groups as well as ionic guests. In LLE, solutes with aromatic structures such as amino acids<sup>28</sup> and phenols or polycyclic aromatic hydrocarbons<sup>29</sup> can engage in π-π interactions, influencing their distribution between the aqueous and organic phases. Sometimes, electron-rich anions including  $\text{SO}_4^{2-}$  and  $\text{NO}_3^-$  can undergo anion-π interaction with electron-deficient aromatic rings which can improve the LLE process of hydrophilic anions contrary to the Hofmeister series. On the other hand, electron-rich aromatic rings can lead to formation of cation-π interaction which allows cations typically alkali and alkaline earth metal cations to be extracted under LLE conditions.

Hence, to optimize the LLE processes, it is essential to understand these supramolecular interactions. Moreover, for the extraction process, influencing these interactions, as well as enhancing the efficiency, requires careful consideration of factors such as the choice of extraction solvent, the addition of phase modifiers, and the control of pH. Researchers often tailor these interactions to achieve the desired separation of components in a mixture during LLE.

## 4. Design of supramolecular extractants

In the supramolecular LLE technique, strongly hydrated inorganic cations and anions are the main solutes of interest. The partition of these ions at the interface of organo-aqueous solvents follows the Hofmeister series which orders ions according to their hydrophobicity and suggests that more hydrophobic ions are easier to extract into the apolar solvent (Fig. 1b).<sup>30</sup> This highlights the importance of developing hydrophobic receptors with adequate recognition sites that can overcome the additional energy barrier for hydrated ions.

Furthermore, for the anionic guests, suitable phase transfer is accompanied by maintaining the charge-neutrality of the LLE system under experimental conditions. Thus, positively charged receptors may give a boost to coulombic interactions with the anions, which allows the formation of a neutral anion-receptor complex that can be more intrinsically soluble in an organic phase.<sup>31</sup> Additionally, charged receptors are also able to eliminate the necessity of transporting the counterion into the organic phase. Thus, this approach has aided in the recognition and extraction of polyvalent oxo-anions such as sulphate, phosphate, dichromate *etc.* Alongside, using the neutral receptors, it is difficult to transport anionic species from an aqueous environment to a nonpolar medium because strong interactions are

observed between water and charge-dense anions. Therefore, receptors must be designed to consist of a large number of binding sites to overcome the hydration effects. In some cases, counterions might also be added to the neutral receptors, which can modulate the extraction process by balancing charge neutrality. Thus, it is convenient for anion extraction through a neutral receptor in terms of ion-pair recognition. Furthermore, a common challenge arises in extracting anions using monotopic receptors in the presence of counterions. This is primarily attributed to the significant energy expenditure required to separate individual anions from their respective counterions.

Therefore, such difficulties can be reduced by developing ion-pair receptors, which provide space for both cations and anions. Additionally, one prebound ion induces the binding of its counterion through a cooperative effect. Such cooperative binding is explained by electrostatic interaction between the bound ions and/or allosteric conformational changes during the binding of the ion-pair. These ion-pair receptors have widely been used as metal salt extractants and solubilizing agents as well as transporters through membranes.<sup>32</sup>

Anions commonly exist in different geometries in nature and sometimes in different forms depending on the pH of the solution (*e.g.*,  $\text{H}_2\text{PO}_4^-$ ,  $\text{HPO}_4^{2-}$ ,  $\text{PO}_4^{3-}$ ). Hence, complementarity between the receptor and anion with regard to size and geometry needs to be addressed to stabilize the anion of interest for effective extraction. Thus, appropriately designed macrocyclic receptors with highly organised structures can efficiently bind a specific anion following geometric complementarity and facilitate LLE.<sup>13</sup> In some cases, cyclodextrins or crown ethers may also pave the way for the selective extraction of specific guest anions or molecules from a solution.<sup>33</sup> Specifically, these molecules can form inclusion complexes with guests, which facilitates the extraction process.

Additionally, controlling the solubility and amphiphilicity of the extractant or receptor is important for compatibility with the extraction system.<sup>34,35</sup> Amphiphilic molecules can interact with both polar and non-polar components, allowing for extraction in various solvent environments. Hence, the design principles behind supramolecular extractants involve a thoughtful combination of structural features, and molecular interaction contributes to optimizing the chemistry of LLE. These design considerations are crucial for achieving high selectivity, efficiency, and adaptability in LLE processes.

In the next part, we will highlight and briefly cover the recent supramolecular hosts that have been developed for the LLE of inorganic anions, alkali metal cations and ion-pairs.

## 5. Removal of anions through LLE

Presently, on the basis of supramolecular hosts designed for the LLE of inorganic anions, two main types of receptors are developed: (a) charged and (b) neutral. In this section, notable examples of success using properly designed cationic or neutral receptor systems for the LLE of anions will be presented. Particularly, the discussion focuses on the design strategy and unique binding properties of receptors in the field in question.





### 5.1. Removal of halides through LLE

The presence of halide ions in water resources can produce undesirable inorganic and organic halide-containing by-products when oxidative treatment is applied during drinking water production. For example, the chlorination or ozonation processes used to effectively kill harmful microorganisms may result in the production of iodoform, brominated phenols, bromate *etc.*, which are potentially carcinogenic and may lead to health concerns.<sup>36</sup> Thus, removal of such halide ions from water is important, where LLE is widely employed due to its usefulness in phase transfer applications.

**5.1.1. Charged receptors for halides.** Fluoride ( $F^-$ ) is an enticing target for anion extraction studies as high levels of  $F^-$  are pernicious to human health.<sup>37</sup> This anion has high hydration enthalpy ( $-465 \text{ kJ mol}^{-1}$ ),<sup>38</sup> making extraction from water a difficult task.

In this scenario, Chiu and Gabbaï reported the extraction of  $F^-$  from water using a cationic borane **R-1**, in a biphasic mixture of  $D_2O$  and  $CDCl_3$  (Fig. 2).<sup>39</sup> The  $F^-$  was captured through hydrogen bond interactions with the methylene proton of the ammonium group of **R-1**, resulting in the formation of a zwitterionic ammonium/fluoroborate complex. This interaction was further validated through solid-state crystal structure analysis and computational studies (Fig. 2). In the solution phase, the endurance of this  $C-H \cdots F-B$  hydrogen bond was confirmed by  $^1H$ ,  $^{19}F$ , and  $^{11}B$ -NMR studies in  $CDCl_3$ . Nevertheless, in the presence of other halides, no evidence of such complex formation was observed. Furthermore, a UV titration conducted in THF/MeOH (75/25 v/v) revealed a higher binding constant ( $5 \times 10^6 \text{ M}^{-1}$ ) for  $F^-$  compared to other halides. The ability of  $F^-$  extraction by **R-1** was assessed through NMR experiments, which revealed that the  $F^-$  adducts were transferred to the organic phase with 82% efficiency. Notably, only the cationic functionality in the borane receptor was able to extract the  $F^-$  because additional hydrogen bonding along with coulombic forces stabilizes the B-F bond against heterolysis. Therefore, these findings imply that cationic borane-based receptors have the capability to overcome the hydration enthalpy of  $F^-$ .

Additionally, in 2011 Das, Ganguly, and co-workers synthesized a phosphonium ( $PPh_3^+$ ) incorporated anthraquinone-based receptor, **R-2**, for the selective colorimetric sensing and

extraction of  $F^-$  (Fig. 2).<sup>40</sup>  $^1H$  and  $^{31}P$  NMR studies of **R-2** with different anions revealed that only  $F^-$  was able to form a 1 : 2 complex with the receptor. This complex formation was assisted by the robust hydrogen bond interaction with the acidic methylene  $CH_2$  protons along with an electrostatic interaction with the cationic  $PPh_3^+$  groups of the receptor, rather than *via* a deprotonation mechanism. Some weak interactions were also found for chloride ( $Cl^-$ ), bromide ( $Br^-$ ), and hydrogen sulphate ( $HSO_4^-$ ), but dihydrogen phosphate ( $H_2PO_4^-$ ) exhibited somewhat stronger interactions. The calculated association constants for  $F^-$  and  $H_2PO_4^-$  were  $2.24 \times 10^6$  and  $8.98 \times 10^4 \text{ M}^{-1}$  respectively in acetonitrile. Hence, with a notable binding constant for  $F^-$ , the receptor exhibited the capability to extract it from water into  $CH_2Cl_2$  or  $CHCl_3$  with 99.3% efficiency, even at  $F^-$  concentration as low as  $2.3 \times 10^{-7} \text{ M}$ . Furthermore, the receptor also demonstrated a similar capability for colorimetric detection of  $F^-$  as compared to the WHO-reported method utilizing sulphonylazodihydroxy naphthalene disulphonic acid, with a lower detection limit of  $3.8 \times 10^{-7} \text{ M}$ . In addition, the authors successfully employed the receptor for a practical application, to extract the  $F^-$  from seawater (Arabian Sea, and Sambhar Lake in India), even in the presence of high concentrations of competing anions.

**5.1.2. Neutral receptors for halides.** In the context of supramolecular LLE employing neutral receptors, Davis invented the term ‘cholapod’ to describe structures where urea or thiourea groups are attached to a steroid skeleton.<sup>41</sup> Using such cholapod-based receptors, Davis, Smith and co-workers reported an extensive study on LLE of the TBA salts of monovalent anions  $Cl^-$ ,  $Br^-$ ,  $I^-$ ,  $NO_3^-$ ,  $AcO^-$ ,  $ClO_4^-$ , and  $EtSO_3^-$ . To achieve selective anion affinity and efficient extraction, a variety of receptors (**R-3 to R-15**) were designed with different kinds and numbers of H-bond donors (3–6) (Fig. 3).<sup>42</sup> Within this group of receptors, **R-14** exhibited a greater affinity for  $Cl^-$  extraction compared to  $Br^-$  from water. In fact, the association constant ( $K_a$ ) was found to be  $1.8 \times 10^{11}$  and  $4.3 \times 10^{10} \text{ M}^{-1}$  for  $Cl^-$  and  $Br^-$ , respectively. The determination of the  $K_a$  values was accomplished by  $^1H$ -NMR integration against an internal standard, 1,1,2,2-tetrachloroethane, in water-saturated  $CDCl_3$ . The high affinity towards  $Cl^-$  was attributed to the formation of effective hydrogen bonding provided by the thiourea groups. The larger number and strategic position of hydrogen bond donors played a crucial role in achieving a well-fitted interaction and enhancing the anion binding, which the authors generalized as the “affinity-selection principle”. This principle may be applied where H-bonding or electrostatic effects dominate anion recognition by similar types of receptors having different binding affinities.

In a later study, Davis, Gale, and co-workers modified the cholapod receptors with squaramide-functionalization to increase the extraction selectivity and efficiency.<sup>43</sup> The inclusion of highly acidic squaramide NH groups in receptor **R-16** bestowed elevated affinities to anions compared to previously reported urea or thiourea-based cholapods (Fig. 4).<sup>44–48</sup> In the case of **R-16a**, the apparent stability constant for  $Cl^-$  was measured to be  $1.2 \times 10^{14} \text{ M}^{-1}$  employing Cram’s extraction method in water-saturated  $CDCl_3$ . In contrast,  $Br^-$ ,  $I^-$ ,  $NO_3^-$ ,

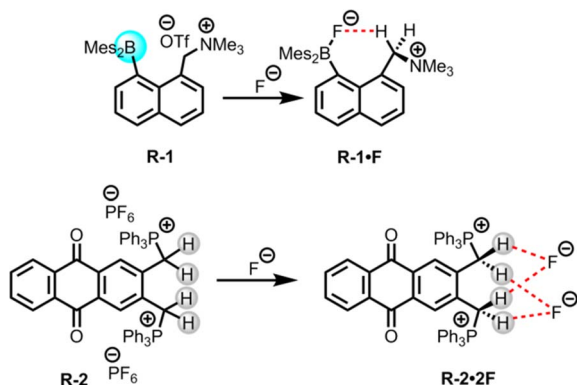


Fig. 2 Chemical structure of the receptors **R-1** and **R-2**.

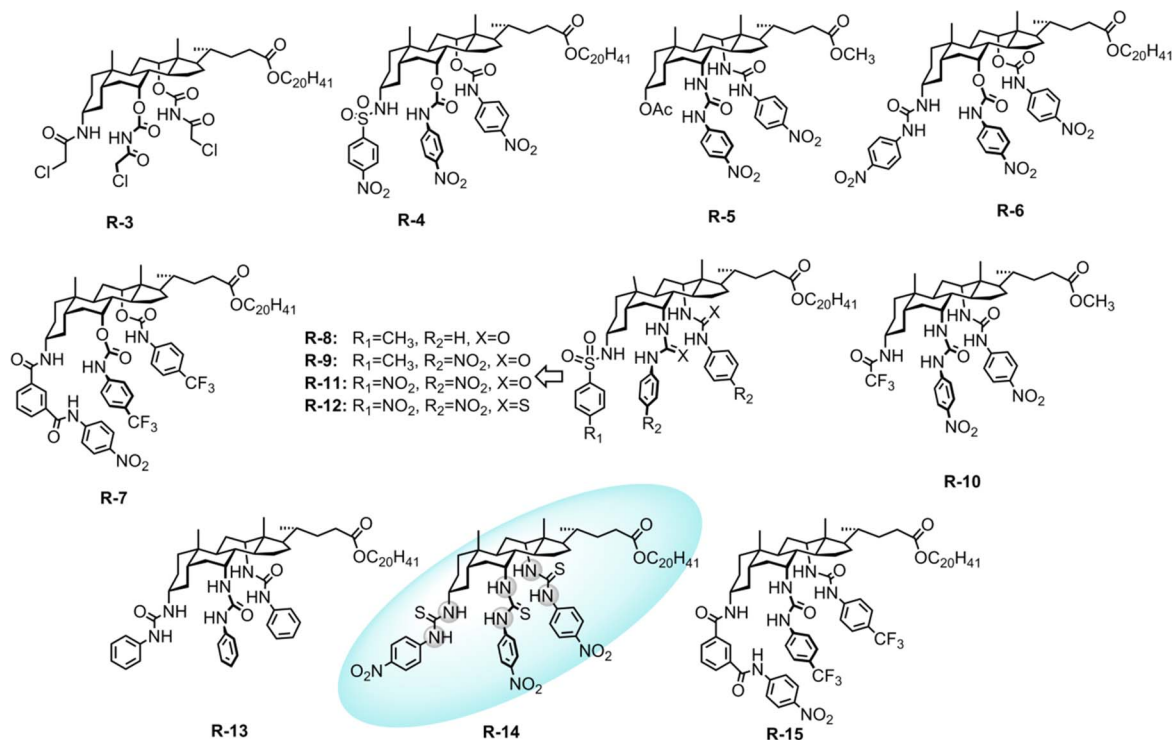


Fig. 3 Chemical structure of the receptors R-3 to R-15.



Fig. 4 Chemical structure of the receptors R-16 and R-20.

$\text{ClO}_4^-$ , and  $\text{EtSO}_3^-$  were seen in the range of  $10^{10}$  to  $10^{13} \text{ M}^{-1}$ . Expectedly, this value is even higher compared to that of **R-14** for selective  $\text{Cl}^-$  recognition by employing cholapod-based receptors. Therefore, the TBA salt of  $\text{Cl}^-$  was readily extracted in the presence of competing monovalent anions from water and transported to the chloroform solvent. Hence, enhancing the effectiveness of hydrogen bonding in receptors can also be achieved without incorporating electrostatic interactions or Lewis-acidic metals.

To develop soluble multivalency receptors for the LLE of halides, Sessler's group reported a calixpyrrole-functionalized organo-soluble polymeric receptor **R-17** (Fig. 4).<sup>49</sup> Prototypical copolymer **R-17** was effectively able to extract  $\text{Cl}^-$  and  $\text{F}^-$  from  $\text{D}_2\text{O}$  to  $\text{CD}_2\text{Cl}_2$ . The extraction ability was assessed through  $^1\text{H}$ -

NMR studies and thermogravimetric analysis. The  $^1\text{H}$ -NMR studies revealed a downfield chemical shift of the pyrrole NH protons upon the addition of  $\text{Cl}^-$  and  $\text{F}^-$ , indicating strong hydrogen bond formation. For **R-17**, extraction efficiency was higher for  $\text{Cl}^-$  than  $\text{F}^-$  or  $\text{H}_2\text{PO}_4^-$ , which is in accord with Hofmeister bias. Interestingly, octamethylcalix[4]pyrrole **R-18** failed to extract  $\text{F}^-$  from water, and  $\text{Cl}^-$  extraction efficiency was also considerably lower compared to that of **R-17**. These results indicate that polymeric receptors enhance the capability for anion extraction through multivalency, while also enabling the tuning of the solubility, stability, and other properties of the extracting agent.

Inspired by the above results Lee *et al.* constructed a gold (Au) nanoparticle decorated with double-armed calix[4]pyrrole receptor **R-19**, which selectively recognized  $\text{F}^-$  with an association constant of  $(1.43 \pm 0.16) \times 10^8 \text{ M}^{-1}$  in  $\text{CH}_2\text{Cl}_2$  (Fig. 4).<sup>50</sup> The core anion recognition subunit of the receptor was calix[4]pyrrole. Additionally, for gold binding, a flexible double anchoring with two thiol-bearing alkyl chains was incorporated. The effective binding between **R-19** and  $\text{F}^-$  was established by the  $^1\text{H}$ -NMR studies. A substantial chemical shift of the pyrrole-NH protons occurred, indicative of the formation of  $\text{N-H}\cdots\text{F}$  hydrogen bonds. The advantage of multivalency of the receptor further enhanced the effective extraction of highly hydrated  $\text{F}^-$  from water into  $\text{CH}_2\text{Cl}_2$ . In contrast, the analogous monomeric calixpyrrole (**R-20**) failed to extract anions under comparable conditions.

A similar result was reported by Akar and Aydogan, based on the tricalix[4]pyrrole and pentacalix[4]pyrrole receptors **R-21** to **R-24** (Fig. 5).<sup>51</sup> These oligomeric calixpyrrole receptors were



Fig. 5 Chemical structure of the receptors R-21 and R-24.

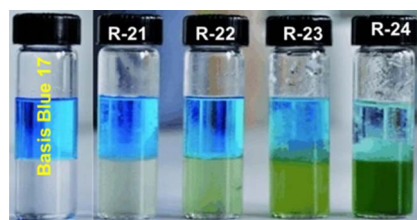


Fig. 6 Visualization of the  $\text{Cl}^-$  extraction by the receptors R-21 to R-24 using Basic Blue 17 (top layer: aqueous solution, bottom layer:  $\text{CH}_2\text{Cl}_2$ ). (Reproduced with permission from ref. 51. Copyright 2018, Wiley.)

capable of extracting the TBA salt of halide ions from a water medium. The extraction capacity was found to be dependent on the number of donor sites present in the receptors. Both **R-21** and **R-22** exhibited the ability to selectively extract  $\text{Cl}^-$  from an aqueous phase into  $\text{CH}_2\text{Cl}_2$ . In contrast, pentacalix[4]pyrrole receptors **R-23** and **R-24** not only extracted the  $\text{Cl}^-$  but were also capable of extracting  $\text{F}^-$ . To visualize the  $\text{Cl}^-$  extraction by the receptors under interfacial aqueous–organic conditions a water-soluble dye, Basic Blue 17, was utilized where  $\text{Cl}^-$  was present as a counter ion (Fig. 6).<sup>52</sup> The result revealed that **R-24** achieved the highest efficiency, with a remarkable 94% extraction compared to other receptors. Furthermore, the enhanced extraction ability of **R-24** was attributed to the cooperative effect of the number of individual calixpyrrole units within its structure, which was established through NMR and thermogravimetric analyses.

Along these lines, in 2018, Jang *et al.* demonstrated triazole containing calix[4]pyrrole based *cis* and *trans* receptors **R-25** and **R-26** respectively (Fig. 7).<sup>53</sup> In comparison to the parent calix[4]pyrrole, both the receptors have effective  $\text{Cl}^-$  binding affinities



Fig. 7 Chemical structure of the receptors R-25 and R-26 and visualization of the  $\text{CH}_2\text{Cl}_2$  phase after extraction of  $\text{Cl}^-$  using Basic Blue 17 through R-25 and R-26. (Reproduced with permission from ref. 53. Copyright 2018, The Royal Society of Chemistry.)

relative to  $\text{Br}^-$  and  $\text{I}^-$  with binding constants of  $1.1 \times 10^5$  and  $2.3 \times 10^4 \text{ M}^{-1}$  for *cis* and *trans* respectively in  $\text{CDCl}_3/\text{CD}_3\text{CN}$  (9/1, v/v) solution. The high binding affinity was rationalised by robust hydrogen bond formation between four pyrrolic N–H and two triazole C–H protons of the receptors. Notably, upon binding with  $\text{Cl}^-$ ,  $^1\text{H}$ -NMR studies demonstrated that the contribution of the  $\text{C–H}\cdots\text{X}$  hydrogen bonding interaction was significantly greater in **R-26** compared to **R-25**. This led to a higher binding constant for the *trans* receptor. The DFT study further unveiled that both receptors interacted with  $\text{Cl}^-$  through cone-shaped conformations. Parenthetically, it is worth noting that both the receptors were able to transfer  $\text{Cl}^-$  into  $\text{CH}_2\text{Cl}_2$  from water-soluble Basic Blue 17 solutions.

Flood and co-workers reported the utility of a polymeric backbone containing receptors **R-27** and **R-28** for the extraction of  $\text{Cl}^-$  from water through  $\text{C–H}\cdots\text{Cl}$  hydrogen bond formation (Fig. 8).<sup>54</sup> The two triazole units of **R-27** adopted both *syn* and *anti*-conformations across the benzene ring, making **R-27** an unorganised receptor. However, **R-28** exhibited a single dominant conformation, which is attributed to intramolecular hydrogen bond interactions. This led to a pre-organized binding site for the anion (Fig. 8). Consequently,  $^1\text{H}$ -NMR revealed that the  $\text{Cl}^-$  binding affinity was higher for **R-28** compared to **R-27**. Furthermore, **R-28** was able to extract  $\text{Cl}^-$  from water into  $\text{CH}_2\text{Cl}_2$ . It was inferred that the high binding and extraction ability was achieved through the effective hydrogen bond formation with the strongly polarized triazole C–H protons.

In continuation of this work, recently Flood, Liu, and co-workers developed a bicyclic cryptand **R-29** with six CH hydrogen-bond donors of triazole groups, which specifically recognized  $\text{Cl}^-$  with a record-breaking attomolar binding affinity ( $10^{17} \text{ M}^{-1}$ ) in wet  $\text{CH}_2\text{Cl}_2$  and high nanomolar affinity ( $10^8 \text{ M}^{-1}$ ) in DMSO.<sup>26</sup> The X-ray crystal structure of the receptor anion complex (**R-29**· $\text{Cl}^-$ ) suggested that the  $\text{Cl}^-$  is encapsulated in the cavity of the **R-29** and stabilized by the nine  $\text{C–H}\cdots\text{Cl}$  hydrogen bonds (Fig. 8). Therefore **R-29** was employed for the extraction of  $\text{Cl}^-$  from water into  $\text{CH}_2\text{Cl}_2$ , achieving up to ~90% efficiency. In addition, larger anions such as  $\text{Br}^-$ ,  $\text{NO}_3^-$ , and  $\text{I}^-$  showed lower binding affinity towards **R-29**, indicating that the receptor displayed anti-Hofmeister behaviour. The receptor was further applied for corrosion inhibition and the result revealed that a film of **R-29** could protect mild steel from corrosion in a brine solution (5.6 M NaCl). This report is undoubtedly



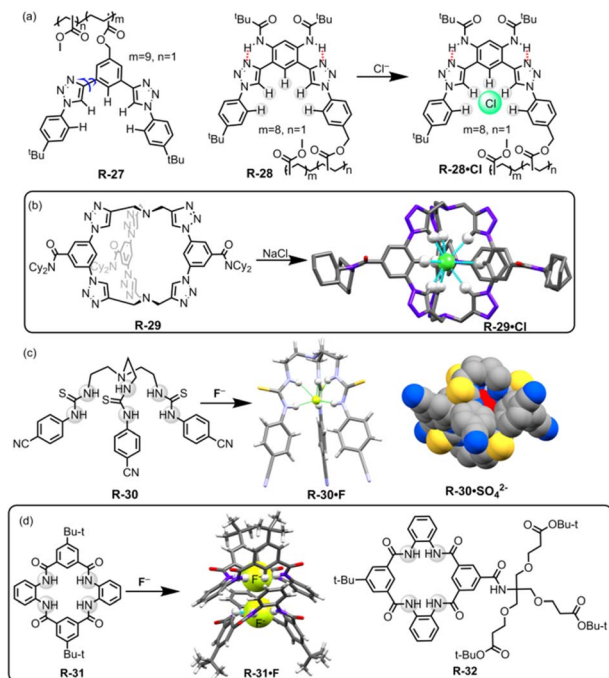


**Fig. 8** (a) Chemical structures of **R-27** and **R-28** (blue arrows indicate the bond rotation). (b)  $\text{Cl}^-$  encapsulation inside the receptor **R-29**. (Data from the Cambridge Crystallographic Data Centre [CCDC # 1533500].<sup>26</sup>) (c) Chemical structures of the receptors **R-30** and crystal structures of **R-30·F** and **R-30·SO<sub>4</sub><sup>2-</sup>**. (Data from the Cambridge Crystallographic Data Centre [CCDC # 875998 and 875999 respectively].<sup>55</sup>) (d) Chemical structures of **R-31** and **32** and crystal structure of **R-31·F**. (Data from the Cambridge Crystallographic Data Centre [CCDC # 1887996].<sup>56</sup>)

a turning point in supramolecular chemistry for the extraction of  $\text{Cl}^-$  that may provide insights into industrial waste purification.

Our group introduced thiourea-based 4-cyanophenyl-substituted tripodal receptor **R-30** for binding of anions both in solution and solid phase and further exploited it for LLE from water (Fig. 8).<sup>55</sup> Isothermal titration calorimetric (ITC) studies revealed that **R-30** exhibited high binding affinity towards spherical  $\text{F}^-$  with a binding constant of  $1.1 \times 10^7 \text{ M}^{-1}$  in  $\text{CH}_3\text{CN}$  compared to other tested tetrahedral oxo-anions ( $\text{H}_2\text{PO}_4^-$  and  $\text{HSO}_4^-$ ). NMR and crystal structure analysis indicated that the  $\text{F}^-$  was encapsulated inside the cavity of the tripodal receptor through the formation of six  $\text{N-H}\cdots\text{F}$  hydrogen-bonding interactions, resulting in a 1:1 complex with distorted trigonal-prismatic geometry. In typical LLE experiments, a  $\text{CHCl}_3$  solution of **R-30** was layered with an aqueous solution of KF containing TBAI as a phase transfer agent, giving rise to an extraction efficiency of  $\sim 70\%$  based on the pure extracted mass. Additionally, **R-30** was also able to extract tetrahedral sulphate with an efficiency of  $\sim 42\%$  by forming a 2:1 tight dimeric capsular assembly. Hence, encapsulating the anions, suitably designed receptors can form a capsular assembly *via* a supramolecular self-assembly process and thereby enhance the extraction efficacy of hydrated anions from competing bulk media.

Recently, Smith and co-workers reported symmetric, neutral tetralactam macrocycle **R-31** containing four amide groups that exhibited anion selectivity towards  $\text{F}^-$  (Fig. 8).<sup>56</sup> In the solution phase,  $^1\text{H}$ -NMR titration for  $\text{F}^-$  demonstrated the formation of a 2:1 (host:guest) complex formed with high association constants ( $K_1 = (5.3 \pm 0.8) \times 10^4 \text{ M}^{-1}$ ,  $K_2 = (3.1 \pm 0.7) \times 10^4 \text{ M}^{-1}$  in  $\text{DMSO-d}_6$ ) compared to other tested anions. The solid-state structure of the  $\text{F}^-$  complex (**R-31·F**) disclosed that the  $\text{F}^-$  occupied the tetralactam cavity through the formation of hydrogen bonds with the four amidic  $-\text{NH}$  and two  $-\text{CH}$  protons. Moreover, the complex also formed a “saddle-shaped” lattice packing as a self-complementary dimer. Inspired by such effective interactions of  $\text{F}^-$  inside the tetralactam cavity, the authors incorporated highly lipophilic groups into that macrocycle to enhance the extraction efficiency of  $\text{F}^-$  from an aqueous solution. Therefore, the macrocycle **R-32** was able to extract  $\text{F}^-$  from water to the  $\text{CH}_2\text{Cl}_2$  phase, even at a low millimolar concentration. Nevertheless, when a mixture of equimolar concentrations of  $\text{F}^-$  and  $\text{Cl}^-$  was present,  $^1\text{H}$  and  $^{19}\text{F}$  NMR indicated that the extraction efficiency of  $\text{F}^-$  was only 4% while for  $\text{Cl}^-$  it became 96%. This discrepancy was attributed to the significant hydration energy difference between  $\text{F}^-$  and  $\text{Cl}^-$ . Therefore, in an environment where there is a highly common occurrence of  $\text{Cl}^-$  the extraction of  $\text{F}^-$  becomes a limitation but the receptors may be used in  $^{18}\text{F}$  radiolabelling technology.<sup>57</sup>  $\text{F}^-$  encapsulation with high binding affinity in the tetralactam cavity could also significantly contribute to the development of fluoride ion batteries (FIBs).<sup>58</sup>

## 5.2. Removal of oxo-anions through LLE

In this section, we will discuss the progress in LLE for oxo-anions through supramolecular approaches. Inorganic oxo-anions such as phosphate, sulphate, pertechnetate, and dichromate are highly toxic in the environment.<sup>59</sup> These oxo-anions contaminate water and soils, mainly through industrial operations and from electroplating. Hence, removal of such ions from the environment is very important but on account of the presence of single/double charge and high hydration enthalpies, extraction from water is difficult.<sup>60–63</sup> Charged and neutral receptors recently reported for oxo-anion extraction are discussed below.

**5.2.1. Charged receptors for oxo-anions.** Metallic oxo-anions like arsenate and dichromates are harmful to living organisms. Contamination of drinking water with arsenate (e.g.,  $\text{H}_2\text{AsO}_4^-/\text{H}_2\text{AsO}_4^{2-}$ ) poses enduring health risks due to its robust binding affinity with sulphhydryl units of proteins. This interference with the reactions of enzymes and proteins can contribute to the development of cancer in the lungs, liver, and lymphatic cells.<sup>63</sup> The oxidising properties of dichromate produce  $\cdot\text{OH}$  and other reactive oxygen species (ROS) in the cell membrane which adversely affects DNA, proteins, and membrane lipids.<sup>64</sup>

Hence, to remove such metallic oxo-anions from a water medium, Bayraktar *et al.* designed tetra-substituted calix[4]arene receptors **R-33** and **R-34** (Fig. 9).<sup>65</sup> These receptors demonstrated the ability to extract arsenic ( $\text{H}_2\text{AsO}_4^-$ ) from water under acidic







Fig. 9 Chemical structure of the receptors R-33 to R-35.

conditions, achieving an extraction efficiency of 81.6% at pH 3.5. **R-33** exhibited high extraction capabilities ( $K_{\text{ex}} = 8.9 \times 10^2 \text{ M}^{-1}$ ), because in an acidic medium, all four pyridyl rings became protonated. This protonation facilitated the formation of a stable host-guest complex *via* electrostatic interactions. Additionally, the amide NH protons formed an effective hydrogen bond with the oxygen atoms of arsenate ( $\text{H}_2\text{AsO}_4^-$ ). At highly acidic pH the stability of  $\text{H}_2\text{AsO}_4^-$  is higher than that of  $\text{H}_2\text{AsO}_4^{2-}$  in water. Therefore, at pH 3.5, **R-33** was capable of facilitating the extraction of  $\text{H}_2\text{AsO}_4^-$  having lower hydration energy than  $\text{H}_2\text{AsO}_4^{2-}$ . In the case of **R-34**, a relatively low 17.7%  $\text{NaH}_2\text{AsO}_4$  extraction ability was observed, which was attributed to the absence of protonatable amine groups and the more electron-donating nature of the furyl groups. Indeed, **R-34** behaved as a ditopic extractant and its  $\text{H}_2\text{AsO}_4^-$  extraction ability was dependent on the binding of  $\text{Na}^+$  within the calixarene cavity. Thus, the formation of an ion-pair complex with the receptor governed the extraction of  $\text{H}_2\text{AsO}_4^-$ . Consequently, these types of receptors offer the opportunity to design the tetra-substituted calix[4]arene architecture for anion-binding with phase-transfer catalysis.

Drawing upon the aforementioned proton-switchable mechanism, Yilmaz *et al.* explored the terpyridin-conjugated calix[4]arene based receptor **R-35** for dichromate extraction (Fig. 9).<sup>66</sup> In the extraction process, a  $\text{CH}_2\text{Cl}_2$  solution of the receptor was agitated with the aqueous solution of  $\text{Na}_2\text{Cr}_2\text{O}_7$  at different pH (1.5–4.5). Upon phase separation, the amount of dichromate ( $\text{HCr}_2\text{O}_7^-$ ) extracted in the organic medium was calculated using UV-Vis analysis. The obtained results revealed that the extraction efficiency depends on the acidity of the solution. Effective extraction of  $\text{HCr}_2\text{O}_7^-$  was not observed at solution pH > 2.5. However, at pH 1.5, the extraction efficiency became ~65% and the  $\text{HCr}_2\text{O}_7^-$  extraction constant  $K_{\text{ex}}$  was found to be  $2.3 \times 10^6 \text{ M}^{-1}$ . Furthermore, the extraction of  $\text{HCr}_2\text{O}_7^-$  by the receptors was not affected in the presence of other competitive anions ( $\text{Cl}^-$ ,  $\text{SO}_4^{2-}$ , and  $\text{NO}_3^-$ ). At low pH, the selectivity and overall effectiveness of **R-35** as an extractant for  $\text{HCr}_2\text{O}_7^-$  were attributed to the presence of proton-switchable

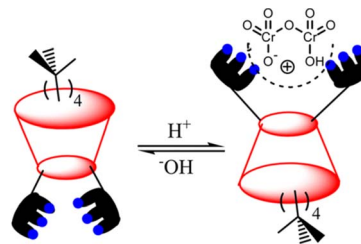


Fig. 10 Schematic representation of interactions between the terpyridin-conjugated calix[4]arene (**R-35**) and  $\text{HCr}_2\text{O}_7^-$ . (Reproduced with permission from ref. 66. Copyright 2014, ACS.)

pyridine moieties (Fig. 10). This led to the formation of a cationic receptor that formed a 1 : 1 complex with  $\text{HCr}_2\text{O}_7^-$  through electrostatic and hydrogen bonding interactions.

Removing the superhydrophilic sulphate ( $\text{SO}_4^{2-}$ ) from water is notoriously difficult due to its high hydration enthalpy ( $-1080 \text{ kJ mol}^{-1}$ ).<sup>60</sup> In this regard, Moyer *et al.* reported simple guanidinium-based receptors **R-36** and **R-37** for the separation of  $\text{SO}_4^{2-}$  from an aqueous medium containing NaCl into 1,2-dichloroethane or isopar L (Fig. 11).<sup>67,68</sup> Noticeably, isopar L is an isoparaffinic hydrocarbon solvent mainly used in industrial extraction processes. During extraction, this low cost diluent plays a significant role in adjusting the receptors' solubility. Moreover, its superior physical properties, such as lower volatility and higher flash point compared to other solvents, make it suitable for use in a radioactive waste processing environment.<sup>69,70</sup> Furthermore, during the extraction experiment the authors utilized a phase-transfer catalyst, a lipophilic quaternary ammonium salt such as Aliquat 336 (methyltrialkyl- $(\text{C}_{8-10})$  ammonium chloride), which increased the  $\text{SO}_4^{2-}$  extraction efficiency by 28 000-fold. It is noteworthy that when utilizing the isopar L solvent for extraction, the separation factor (SF) for  $\text{SO}_4^{2-}$  over  $\text{Cl}^-$  was found to be >1, which is rarely observed in the literature. The main driving force for effective binding and separation of  $\text{SO}_4^{2-}$  was the coulombic interaction with the guanidinium-based receptors, along with the formation of a 1 : 2 complex. The  $\text{SO}_4^{2-}$  distribution ratio for such a stoichiometric complex hinged on the extractant concentration which was influenced by the charge discrepancy between the  $\text{SO}_4^{2-}$  and  $\text{Cl}^-$  during the ion exchange process. Additionally, **R-37** showed better selectivity and high extraction power compared to **R-36**. This was attributed to the formation of reverse-micelles of the sulphate complex of **R-37** in solution, which was further supported by Karl Fischer titrations and small angle X-ray scattering experiments.

The aforementioned extraction of  $\text{SO}_4^{2-}$  through LLE clearly illustrated that phase-transfer catalysts such as Aliquat 336 abbreviated to A336N can play a pivotal role in overcoming the Hofmeister bias. The primary function of this catalyst involves an anion exchange mechanism between  $\text{Cl}^-$  of the extractant and the targeted anion ( $\text{SO}_4^{2-}$ ,  $\text{HPO}_4^{2-}$  *etc.*) of the feed solution. The structure of Aliquat 336 and reaction involved during salt exchange are depicted in Fig. 12. In addition, methyl(*n*-octyl,*n*-decyl)ammonium nitrate and *N,N*-bis(2-ethylhexyl)guanidine (**LIX 79**) also behaved as classic phase-transfer catalysts.<sup>71,72</sup>

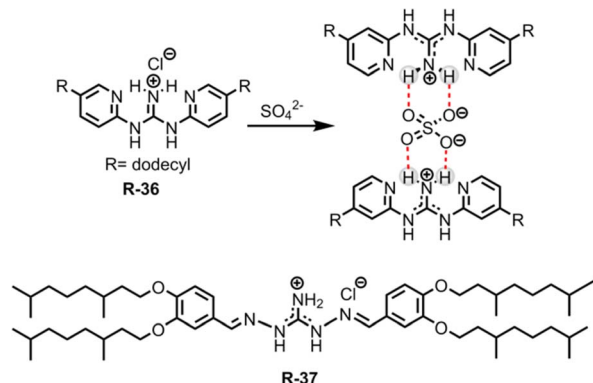


Fig. 11 Chemical structures and  $\text{SO}_4^{2-}$  binding with **R-36** and **R-37**.



Fig. 12 Representation of the anion exchange mechanism for univalent anions with chloride and the structures of **A336N** and **LIX 79**.

Particularly, in the case of highly hydrated anions, like sulphate and phosphate, during LLE, a third phase is developed by this catalyst. At the critical point of phase splitting, the amount of water in the organic phase is correlated with the targeted anion's hydration energy, thereby facilitating the extraction process. Furthermore, phase transfer catalysts not only maintain the charge neutrality but also improve the stability of the targeted anion–receptor complex in less polar solvents. Nevertheless, they enhanced the exchange kinetics of LLE. Using such a phase-transfer catalyst approach Sessler and Moyer successfully reported several macrocyclic-based receptors for anion extraction.<sup>15,16,73</sup>

**5.2.2. Neutral receptors for oxo-anions.** For the removal of sulphate, Sessler, Moyer, and colleagues investigated the extraction behaviour of fluorinated calixpyrroles **R-38** and **R-39** and tetraamide macrocycles **R-40** and **R-41** in the presence of a phase transfer catalyst (Fig. 13).<sup>74</sup> The extraction studies by these receptors demonstrated that the  $\text{SO}_4^{2-}$  extraction efficiency significantly increased when Aliquat 336 was introduced into the organic phase. Among the receptors, **R-39** and **R-41** displayed the maximum extraction ability towards  $\text{SO}_4^{2-}$  which was attributed to strong binding through more NH hydrogen-bond donors and lipophilicity effects.

In subsequent works,<sup>75,76</sup> the authors described the effectiveness of adding Aliquat 336 to aid  $\text{SO}_4^{2-}$  extraction by the receptor **R-18**, even when  $\text{NaNO}_3$  was present in excess. Interestingly, it was found that despite the higher binding capacity, **R-38** showed lower efficiency for removing  $\text{SO}_4^{2-}$  than **R-18**. This finding was observed as in the presence of Aliquat 336, **R-18** acted as a ditopic receptor which helped to stabilize the **R-**



Fig. 13 (a) Chemical structure of the receptors **R-38** to **R-41**. (b) Representation of  $\text{SO}_4^{2-}$  binding with **R-18**.

**18·SO<sub>4</sub><sup>2−</sup>** complex (Fig. 13). The solid-state structure revealed that  $\text{SO}_4^{2-}$  bound to the cavity through the oxygen atom while the cationic part of **A336N** concurrently bound within the cup-like portion of **R-18**. In addition, if the size of the long-chain quaternary ammonium increased the extraction efficiency decreased due to a poor fit with the “cup”.

In a further report, the same group demonstrated bipyrrole-strapped calix[4]pyrrole-based receptors **R-42** and **R-43** with enhanced extraction efficiency of  $\text{SO}_4^{2-}$  from water (Fig. 14).<sup>77</sup> It was also found that the  $\text{SO}_4^{2-}$  extraction capacity of the receptors was significantly increased in the presence of excess  $\text{NaCl}$ , as well as upon using the co-extractant **A336N**. In fact, **A336N** stabilized the sulphate–receptor complex by the formation of  $\text{C-H}\cdots\pi$  interactions between one of the methyl groups of **A336N** and the  $\pi$ -faces of the pyrroles. These methyl groups also concomitantly bound to the  $\text{SO}_4^{2-}$  which significantly improved the ion pairing effects (Fig. 14). Hence, the formation of a higher-order complex improved the stability of  $\text{SO}_4^{2-}$  in the organic phase. **R-43** exhibited a higher extraction efficiency compared to **R-42**, with distribution ratios of 0.013 and 0.00061 respectively. The higher performance of **R-43** was attributed to the fact that the divergent NH vectors of the

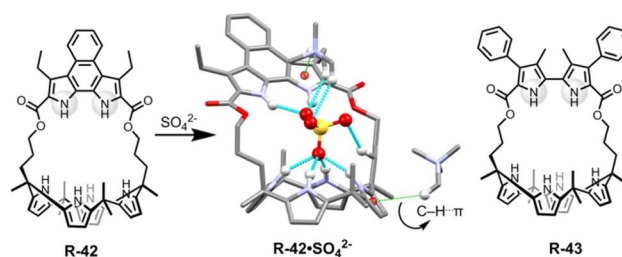


Fig. 14 Chemical structure of the receptors **R-42** and **R-43** and crystal structure of **R-42·SO<sub>4</sub><sup>2−</sup>**. (Data from the Cambridge Crystallographic Data Centre [CCDC # 1017884 (ref. 77)].)



bipyrrole subunit were able to better encapsulate the  $\text{SO}_4^{2-}$  by generating strong hydrogen bond interactions with the two oxygen atoms.

Theoretical analysis has established that the binding of  $\text{SO}_4^{2-}$  can be stabilized by the saturated 12 coordinated tetrahedral cavity within the receptor, facilitated by organized hydrogen bonds.<sup>78</sup> In this regard, Li, Wu, and co-workers achieved hexaurea-based tripodal receptor **R-44** for the effective extraction of  $\text{SO}_4^{2-}$  in the presence of nitrate-rich mixtures (Fig. 15).<sup>79</sup> The X-ray crystal structure demonstrated that the receptor was capable of encapsulating  $\text{SO}_4^{2-}$  through effective hydrogen-bonding interactions with NH protons, resulting in a saturated twelve-coordinate tetrahedral geometry. Therefore, the  $\text{SO}_4^{2-}$  binding ability became quite high ( $K_a > 10^4 \text{ M}^{-1}$ ) compared to other tested anions. This finding encouraged the authors to investigate the LLE of  $\text{SO}_4^{2-}$  using NMR and gravimetric techniques. <sup>1</sup>H-NMR studies revealed that **R-44** efficiently extracted the  $\text{SO}_4^{2-}$  into the organic phase ( $\text{CDCl}_3$ ) from a nitrate-rich aqueous solution by an ion exchange method with 95% extraction efficiency. Furthermore, once extracted,  $\text{BaCl}_2$  was loaded to the organic phase for the precipitation of  $\text{SO}_4^{2-}$  as  $\text{BaSO}_4$  allowing the extractant to be recycled for reuse.

In another recent report, to explore the  $\text{SO}_4^{2-}$  binding capability, the same research group of Zhao, Wu, and co-workers elucidated a class of C3 symmetric tripodal hexaurea-based receptors **R-44** to **R-46** for the separation of  $\text{SO}_4^{2-}$  from water by the LLE method (Fig. 15).<sup>80</sup> The receptor's affinity for  $\text{SO}_4^{2-}$  binding was controlled by altering the terminal

substituents present in the receptor, which contributed to the formation of robust hydrogen bonds and secondary C-H $\cdots\pi$  interactions. Therefore, the tendency for stronger binding as well as the better potential for  $\text{SO}_4^{2-}$  removal followed the order **R-44** > **R-45** > **R-46**. To enhance the  $\text{SO}_4^{2-}$  extraction efficiency of the receptors, A336N was used instead of TBACl. Furthermore, <sup>1</sup>H-NMR and ICP-MS studies revealed that the extraction efficiency for **R-44** became ~95% while it was 86% and 78% for **R-45** and **R-46**, respectively. The extraction equilibrium constants ( $K_{\text{ex}}$ ) were also calculated for the receptors and were found to be  $2.4 \times 10^9$ ,  $1.5 \times 10^9$ , and  $7.8 \times 10^8 \text{ M}^{-1}$  for **R-44**, **R-45**, and **R-46** respectively. A weak C-H $\cdots\pi$  interaction between the phenyl spacers and terminal hexyl groups was observed for the hydrophobic receptor **R-46** which enabled the receptor to be repeatedly used for the extraction and release of the  $\text{SO}_4^{2-}$  in an acidic medium by converting  $\text{SO}_4^{2-}$  to  $\text{HSO}_4^-$ . Moreover, Cram's U-tube experiments employing **R-46** illustrated the dynamic transport of  $\text{SO}_4^{2-}$  and ~70% of sulphate was transported from the source phase to the receiving phase in 3 days. The authors asserted that, to date, this represents the most efficient report on sulphate transport efficiency. Eventually, the designing principles of such receptors represent a paradigm that can aid in enhancing our understanding and tailoring the receptors for selective  $\text{SO}_4^{2-}$  separation.

In 2012, our group used a urea-based receptor **R-47** for the LLE of  $\text{SO}_4^{2-}$  from an aqueous medium (Fig. 16).<sup>81</sup> It is noteworthy to mention that the receptor itself was not able to extract  $\text{SO}_4^{2-}$  due to solubility issues. However, pre-encapsulation of  $\text{CO}_3^{2-}$  with **R-47** solubilised the receptor, enabling it to effectively extract  $\text{SO}_4^{2-}$  through an anion exchange method. This finding can be explained by considering that  $\text{SO}_4^{2-}$  has a lower hydration energy ( $\Delta G_{\text{h}} = -1080 \text{ kJ mol}^{-1}$ ) as well as a higher association constant for **R-47** compared to  $\text{CO}_3^{2-}$  ( $K_a = 4.68 \times 10^4$  and  $1.17 \times 10^4 \text{ M}^{-1}$  respectively, in dry DMSO). Despite the presence of other competing oxo-anions of TBA salts like  $\text{H}_2\text{PO}_4^-$  and  $\text{NO}_3^-$ , the **R-47**· $\text{CO}_3^{2-}$  complex demonstrated selective extraction of  $\text{SO}_4^{2-}$  from aqueous media. In the extraction process, a  $\text{CHCl}_3$  solution of **R-47**· $\text{CO}_3^{2-}$  was agitated with an aqueous solution of  $\text{K}_2\text{SO}_4$ . The salt exchange mechanism was elucidated using a phenolphthalein indicator, and the pink coloration of the aqueous phase indicated the exchange of  $\text{CO}_3^{2-}$  in the water medium. Additionally, NMR analyses of the organic phase suggested 99%  $\text{SO}_4^{2-}$  complexation with **R-47**. Moreover, for the gravimetric analysis and to facilitate the reuse of the receptor,  $\text{BaCl}_2$  was added to the organic phase to precipitate the extracted  $\text{SO}_4^{2-}$  as  $\text{BaSO}_4$ , confirming the extraction of  $\text{SO}_4^{2-}$ .

In a subsequent report, our research team introduced another tripodal scaffold with the 3-cyanophenyl-substituted receptor **R-48** (Fig. 16).<sup>82</sup> This receptor also formed a 2:1 dimeric capsular assembly of  $\text{CO}_3^{2-}$  by capturing atmospheric carbon dioxide ( $\text{CO}_2$ ) from a basic DMSO solution. The outstanding solubility of **R-48**· $\text{CO}_3^{2-}$  in  $\text{CHCl}_3$  had been harnessed for the selective LLE of  $\text{CrO}_4^{2-}$ ,  $\text{SO}_4^{2-}$ , and  $\text{S}_2\text{O}_3^{2-}$  ions from water through an anion-exchange metathesis process. All of these three anions were capable of forming an almost identical 2:1 (H-G) dimeric capsular assembly. However, the **R-**



Fig. 15 (a) Chemical structure of the receptor **R-44** and crystal structure of **R-44**· $\text{SO}_4^{2-}$ . (Data from the Cambridge Crystallographic Data Centre [CCDC # 784518 (ref. 79)].) (b) Chemical structures of the receptors **R-44** to **R-46** and  $\text{SO}_4^{2-}$  binding crystal structure of **R-46**. (Data from the Cambridge Crystallographic Data Centre [CCDC # 2206147].<sup>80</sup>)







Fig. 16 (a) Chemical structure of the receptor **R-47**. (b) Representation of the assembly of **R-47·CO<sub>3</sub><sup>2-</sup>**. (c) Visualization of **SO<sub>4</sub><sup>2-</sup>** extraction using phenolphthalein through the **R-47·CO<sub>3</sub><sup>2-</sup>** complex. (Reproduced from ref. 81. Copyright 2012, The Royal Society of Chemistry.) (d) Schematic representation of LLE by **R-48** (Reproduced from ref. 82. Copyright 2014, Wiley.) (e) Chemical structures of the receptors **R-49** and **R-50**. Illustration of the general setup for the U-tube experiments used to test the ability of **R-50** to act as a carrier for **SO<sub>4</sub><sup>2-</sup>**. (Reproduced from ref. 83. Copyright 2020, The Royal Society of Chemistry.)

**48·CO<sub>3</sub><sup>2-</sup>** complex failed to extract **H<sub>2</sub>PO<sub>4</sub><sup>-</sup>**, **HAsO<sub>4</sub><sup>2-</sup>** and **F<sup>-</sup>** ions. The **CrO<sub>4</sub><sup>2-</sup>** extraction was confirmed by the <sup>53</sup>Cr-NMR and UV-Vis studies. Moreover, the extraction of the aforementioned anions by the carbonate complex was supported by the NMR, IR, PXRD, and X-ray diffraction analyses. Quantification through weighing the extracted complexes revealed an extraction efficiency of ~90% for the three anions. Furthermore, quantitative estimations through gravimetric analysis, by treating **BaCl<sub>2</sub>** to form **BaCrO<sub>4</sub>** and **BaSO<sub>4</sub>**, demonstrated an efficiency of >90% for **CrO<sub>4</sub><sup>2-</sup>** and **SO<sub>4</sub><sup>2-</sup>**. Particularly, during the extraction of **CrO<sub>4</sub><sup>2-</sup>** in the presence of **SO<sub>4</sub><sup>2-</sup>** ions, the UV-Vis spectra analysis indicated ~50% extraction capacity for **CrO<sub>4</sub><sup>2-</sup>** ions. Moreover, in the separation of **SO<sub>4</sub><sup>2-</sup>** for the nuclear waste treatment, the pH of the medium is a crucial factor. Consequently, in the presence of 5 equiv. of **NO<sub>3</sub><sup>-</sup>**, the **48·CO<sub>3</sub><sup>2-</sup>** complex demonstrated excellent **SO<sub>4</sub><sup>2-</sup>** extraction capability at pH 12.5, whereas **R-47·CO<sub>3</sub><sup>2-</sup>** could only achieve extraction up to pH 10.5. Interestingly, this marks the inaugural report on the LLE of **CrO<sub>4</sub><sup>2-</sup>** and **S<sub>2</sub>O<sub>3</sub><sup>2-</sup>** ions from water using an anion-exchange technique.

Most recently, Jolliffe *et al.* developed squaramide-based macrocycles **R-49** and **R-50**, which were able to extract **SO<sub>4</sub><sup>2-</sup>** from the aqueous phase into **CHCl<sub>3</sub>**, via a nitrate ion exchange mechanism with the assistance of lipophilic tetraalkylammonium cations (Fig. 16).<sup>83</sup> <sup>1</sup>H-NMR titrations in **CDCl<sub>3</sub>** revealed that **R-50** can bind to **TBASO<sub>4</sub>** with  $K_a > 10^4 \text{ M}^{-1}$ . Therefore, in a wide pH range (pH 3.2–9.4), **R-50** was able to transport the **SO<sub>4</sub><sup>2-</sup>** across a bulk **CHCl<sub>3</sub>** membrane in a Cram U-tube experiment. Furthermore, to recycle the receptor, the authors employed the aforementioned method for the precipitation of **SO<sub>4</sub><sup>2-</sup>** as **BaSO<sub>4</sub>**. The amount of sulphate extracted from the precipitated **BaSO<sub>4</sub>** was calculated by gravimetric analysis and inductively coupled plasma mass spectrometry (ICP-MS) experiments. In contrast to sodium salts, the lipophilic tetrabutylammonium salt of **SO<sub>4</sub><sup>2-</sup>** had been extracted by **R-50**. The extraction ability for the **SO<sub>4</sub><sup>2-</sup>** was also evaluated in the presence of nitrate ions by the metathesis method. NMR analysis of the organic phase indicated that the NH protons of **R-50** were involved in the extraction of **SO<sub>4</sub><sup>2-</sup>**. Moreover, in acidic medium (pH 3.2), the **SO<sub>4</sub><sup>2-</sup>** extraction affinity was increased due to the protonation of the isonicotinamide part of the receptor. Moreover, **R-50** possesses the capability to transport **SO<sub>4</sub><sup>2-</sup>**, signifying its potential for usefulness for nuclear-waste treatment.

For the extraction of polyvalent oxo-anions, urea-based neutral tripodal receptor **R-51** was reported by Dey and co-workers, which exhibited selective encapsulation and extraction properties for **HPO<sub>4</sub><sup>2-</sup>** from water (Fig. 17).<sup>84</sup> <sup>1</sup>H- and <sup>31</sup>P-NMR, and crystal structure analysis revealed that

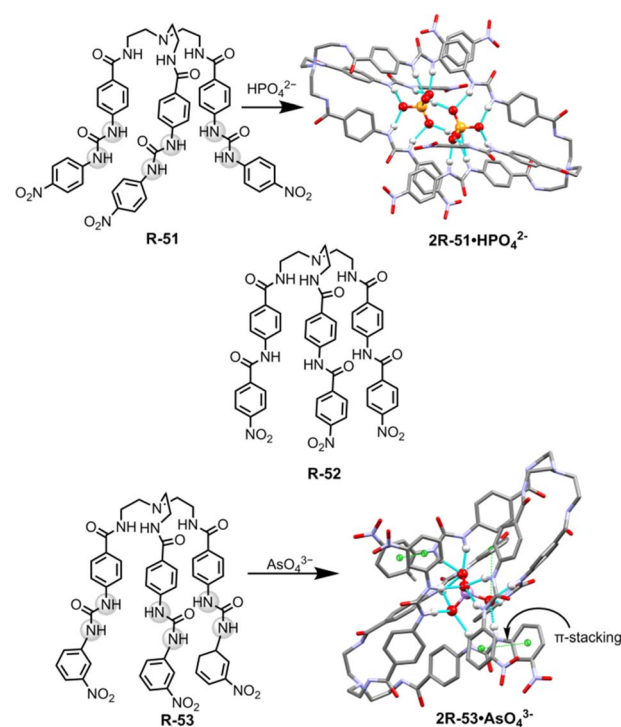


Fig. 17 Chemical structure of the receptors **R-51** to **R-53** and crystal structures of **2R-51·HPO<sub>4</sub><sup>2-</sup>** and **2R-53·AsO<sub>4</sub><sup>3-</sup>** (data from the Cambridge Crystallographic Data Centre [CCDC # 2008261 and 2172773 respectively]<sup>[84,85]</sup>).

encapsulation of  $\text{HPO}_4^{2-}$  involved the formation of six hydrogen bond interactions with the three urea groups present in the receptor. The formation of a hydrogen-bonded capsule by the dimeric association between receptors and  $\text{HPO}_4^{2-}$  was also a strong reason for the selectivity (Fig. 17). Therefore, receptors can efficiently extract  $\text{HPO}_4^{2-}$  from water to  $\text{CH}_2\text{Cl}_2$  even in the presence of different competitive anions ( $\text{F}^-$ ,  $\text{CN}^-$ ,  $\text{CH}_3\text{COO}^-$ , and  $\text{HSO}_4^-$ ) as indicated by  $^1\text{H}$  and  $^{31}\text{P}$ -NMR analysis. The authors also suggested that at neutral pH  $\text{H}_2\text{PO}_4^-$  is in equilibrium with  $\text{HPO}_4^{2-}$  ( $\text{p}K_a$  7.21) whereas at high pH only  $\text{PO}_4^{3-}$  is present. Thus,  $\text{K}_3\text{PO}_4$  was used in the extraction experiment. Moreover, another tris-amide-based receptor **R-52** was unable to extract the anions due to the absence of sufficient hydrogen bond donors inside the receptor cavity to stabilise an anion.

Additionally, in 2022, the same group crafted an *N*-bridged urea-based tripodal receptor **R-53** which was able to selectively extract arsenate ( $\text{AsO}_4^{3-}$ ) from water in the presence of phosphate, despite having close similarities in ionic charge, thermodynamic radii,  $\text{p}K_a$  values, and hydration energies (Fig. 17).<sup>85</sup> The high selectivity for arsenate was exhibited through its encapsulation inside the receptor, facilitated by eleven hydrogen bond interactions and the formation of a  $\pi$ -stacked rigid capsular assembly. The extraction experiments were executed at different pH (5.5, 7.4, 9.5, and 11). Notably, only under basic pH conditions (7.4, 9.5, and 11)  $\sim 90\%$  of arsenate was successfully extracted in the organic phase by **R-53**, employing an anion exchange method using  $(n\text{-Bu}_4\text{N}^+)\text{OH}^-$ . Nevertheless, arsenate extraction was not possible at acidic pH 5.5. Thus, the major disadvantage of the charged receptor **R-33**, *i.e.*, extraction ability only in an acidic medium, can be overcome by the neutral receptor **R-53**. However, there remains a need for the development of pH-independent receptors to facilitate arsenic extraction.

Radioactive wastewater treatment is one of the most pressing issues in current research relating to the LLE of anions. Therefore, researchers have become interested in the efficient removal of radioactive and toxic inorganic metal oxo-anions such as  $^{99}\text{TcO}_4^-/\text{ReO}_4^-$  from wastewater.<sup>86–88</sup> In this context, recently, Gale and co-workers developed a superphane receptor **R-54** which contains six amide-NH and six secondary NH-units that selectively encapsulated and efficiently extracted  $\text{ReO}_4^-$  from water (Fig. 18).<sup>89</sup>  $^1\text{H}$ -NMR studies with  $\text{ReO}_4^-$  revealed that  $\text{ReO}_4^-$  was able to form 18 strong hydrogen bonds leading to

a binding constant ( $K_a$ ) of  $(5.62 \times 0.15) \times 10^3 \text{ M}^{-1}$  in  $\text{CDCl}_3/\text{CD}_3\text{OD}$  (1 : 1, v/v). In addition, the single crystal structure of the  $\text{ReO}_4^-$  complex suggested the encapsulation of  $\text{ReO}_4^-$  inside the cavity of the receptor by 1 : 1 complexation. Most importantly, in LLE studies within a  $\text{CHCl}_3$ -water medium, by employing **R-54**, a remarkable 99.99%  $\text{ReO}_4^-$  extraction was accomplished, where the initial perrhenate concentration was  $\sim 0.003 \text{ M}$ . Additionally, after careful separation of the aqueous phase, further consecutive multiple extractions (1 to 7 cycles) of that aqueous solution were conducted. ICP-MS analysis revealed a sharp decrease in  $\text{ReO}_4^-$  concentration, reaching  $4.40 \times 10^{-6} \text{ M}$ . Astonishingly, with an increase in the number of extraction cycles up to 10, there was a notable improvement in extraction efficiency, ultimately reducing the perrhenate concentration to less than  $\sim 3.67 \times 10^{-8} \text{ M}$ . Even in the presence of high concentrations of other competing anions such as  $\text{SO}_4^{2-}$ ,  $\text{H}_2\text{PO}_4^-$ , and  $\text{MoO}_4^-$ , the  $\text{ReO}_4^-$  extraction ability was not significantly affected. Interestingly, at lower pH the receptor showed high extraction ability but at higher pH the extraction ability was reduced because  $\text{ReO}_4^-$  was extracted in the form of  $[\text{R-54} \cdot 2\text{H}^+ \cdot \text{ReO}_4^-]$ . Therefore, this study will be expected to boost the designing of the receptors in the future for controlled binding, release, and transport of the targeted anion for biological and industrial purposes.

**5.2.3. Coordination complex-based receptors for oxo-anions.** To extract oxo-anions, instead of using conventional organic covalent receptors, coordination complex-based receptors obtained by employing self-assembly approaches are promising in current supramolecular chemistry.

The Nitschke group exploited the extraction capability of a coordination cage under an interfacial state. In this regard, they adopted the azaphosphatane unit, which was able to bind anions through hydrogen bonding along with electrostatic interaction. The  $\text{Fe}_4\text{L}_4$  cage **R-55** was synthesized *via* an anionic template-directed self-assembly process (Fig. 19).<sup>90</sup> For **R-55** with lipophilic counterion  $\text{BARF}_4^-$ , the relatively weakly bound template  $^n\text{BuBF}_3^-$  (*n*-butyltrifluoroborate) was able to exchange easily with  $\text{ReO}_4^-$ . As a consequence, 97% of  $\text{ReO}_4^-$  was extracted from water to nitromethane in the presence of competing anions ( $\text{F}^-$ ,  $\text{Cl}^-$ ,  $\text{Br}^-$ ,  $\text{I}^-$ ,  $\text{SO}_4^{2-}$ ,  $\text{ClO}_4^-$ ,  $\text{NO}_3^-$ ,  $\text{BF}_4^-$ ,  $\text{H}_2\text{PO}_4^-$ , and  $\text{AcO}^-$ ) which was confirmed *via*  $^1\text{H}$ -NMR. In relatively less polar ethyl acetate, the  $\text{ReO}_4^- \subset \text{R-55}$  was disassembled to release the extracted  $\text{ReO}_4^-$  which could be reassembled again in acetonitrile with the help of the  $^n\text{BuBF}_3^-$  template. Furthermore, a reverse extraction of  $\text{ReO}_4^-$  from the organic to the aqueous phase was also achieved with a water-soluble receptor with the  $\text{SO}_4^{2-}$  counterion. Therefore, for repeated oxo-anion extraction through the assembly and disassembly process in different solvents, these metallacages may be advantageous compared to conventionally used covalent receptors.

On the other hand, Huang *et al.* reported  $\text{ReO}_4^-$  extraction with functionalized electron-deficient paracyclophane (PCP) supramolecular host **R-56**. In contrast to the electron-rich PCP moiety, the embedding of the ruthenium unit *via*  $\pi$ -metallation generated a polymetalated PCP which exhibited better regioselectivity as well as efficiency for anion binding (Fig. 19).<sup>91</sup> As



Fig. 18 Structure of receptor **R-54** and the corresponding  $\text{ReO}_4^-$  binding crystal. (Data from the Cambridge Crystallographic Data Centre [CCDC # 2111255].<sup>89</sup>)





Fig. 19 Chemical structure of the receptors **R-55** to **R-60**, crystal structure of the **R-56·ReO<sub>4</sub>** complex (data from the Cambridge Crystallographic Data Centre [CCDC # 1951588]<sup>91</sup>) and self-assembled structure of  $[(\text{R-60a})_2\text{Cu}_3(\text{SO}_4)]^{4+}$ . (Reproduced from ref. 93. Copyright 2020, Wiley-VCH GmbH.)

evident from  $^1\text{H-NMR}$ , **R-56** preferentially bound  $\text{ReO}_4^-$  over other tested anions both in  $\text{D}_2\text{O}$  and  $\text{CD}_3\text{NO}_2$  solvents, further supporting the fact that the extraction of  $\text{ReO}_4^-$  was not significantly hampered by other oxo-anions including  $\text{SO}_4^{2-}$ ,  $\text{NO}_3^-$ ,  $\text{ClO}_4^-$ , etc. At the interface, about 79% of  $\text{ReO}_4^-$  had been extracted from  $\text{D}_2\text{O}$  to  $\text{CD}_3\text{NO}_2$ , when the receptor concentration was maintained at 0.004 M. Furthermore, the tri-metalated species **R-56** bound  $\text{ReO}_4^-$  in a tweezers-like manner through anion- $\pi$  interaction as evidenced from the solid state structure. On that account, this study could also be expanded to anion encapsulation to facilitate the extraction process by increasing the number of benzene rings in PCP with further modification in  $\pi$ -metalation through the group-VIII transition elements.

For the extraction of oxo-anions like phosphate and carboxylate our group has utilized the ruthenium-coordinated receptor **R-57** (Fig. 19).<sup>92</sup> Considerable hydrogen bonding was observed in the case of phosphates, involving the urea  $-\text{NH}$  and the triazole  $\text{CH}$  protons. For carboxylates, only the urea  $-\text{NH}$  participated, as evidenced by a significant downfield shift in the  $^1\text{H-NMR}$  spectrum in  $\text{DMSO}-d_6$ . Further investigations on LLE following several NMR approaches manifested that **R-57** could extract  $\text{H}_2\text{PO}_4^-$ ,  $\text{CH}_3\text{COO}^-$  and  $\text{PhCOO}^-$  from water to  $\text{CHCl}_3$  with 28%, 74%, and 80% efficiency respectively. The notable role of urea in the extraction of  $\text{CH}_3\text{COO}^-$  and  $\text{PhCOO}^-$  was demonstrated through the negative extraction results when using the receptor **R-58** without urea connectivity.

Recently, Rice and co-workers reported the LLE of phosphate selectively by self-assembly driven copper complexes. In this regard, **R-59a** and **R-60a** were synthesized and can form trinuclear copper complexes.<sup>93</sup> This trinuclear assembly in host-guest complexation was confirmed by a single crystal of a  $\text{SO}_4^{2-}$  encapsulated complex  $[(\text{R-60a})_2\text{Cu}_3(\text{SO}_4)]^{4+}$ . Further, **R-59b** and **R-60b** with aliphatic hexyl esters were prepared to increase the solubility of the assemblies in an organic solvent. The initial dark-yellow or pale-yellow  $\text{CH}_2\text{Cl}_2$  solution of  $\text{Cu}(\text{OTf})_2$  and **R-59b** or **R-60b** changed to lime green upon exposure to an aqueous  $\text{NaH}_2\text{PO}_4$  solution indicating phosphate binding in the cavity which was further supported by UV-Vis studies (Fig. 19). Based on ion chromatography, a stoichiometric amount of hosts  $[(\text{R-59b})_2\text{Cu}_3]^{6+}$  and  $[(\text{R-60b})_2\text{Cu}_3]^{6+}$  can extract around 82 and 76% of  $\text{H}_2\text{PO}_4^-$  respectively from water. In addition, such assemblies were formed selectively in the case of sulphate and phosphate rather than chloride and nitrate salts. While using  $\text{Na}_2\text{HPO}_4$ , a slightly higher phosphate preference was observed with  $[(\text{R-60b})_2\text{Cu}_3]^{6+}$  compared to  $[(\text{R-59b})_2\text{Cu}_3]^{6+}$ . The rigid small cyclohexyl spacer in **R-60** induced shorter  $\text{Cu}\cdots\text{anion}$  and  $\text{NH}\cdots\text{anion}$  distances, thus creating a cavity that was favourable for selective phosphate binding over other anions.

## 6. Removal of alkali metals through LLE

Contamination of water with highly concentrated alkali metal salts makes it undrinkable. In particular, the diffusion of radioactive caesium (Cs) from the testing of weapons and the nuclear industry has caused a major environmental problem.<sup>94</sup> To avoid these environmental as well as health problems, it is important to remove alkali metal ions from an aqueous solution.

In this context, Akkus *et al.* prepared a series of calix[4]-oxa-crown and calix[4]-thia-crown derivatives **R-61** to **R-64**, where nitrile, amino, and oxime groups attached at the lower rim of the calixcrown (Fig. 20).<sup>95</sup> Among the receptors, **R-61a** exhibited a preference for extracting  $\text{Na}^+$  over  $\text{K}^+$  owing to a perfect fit in the cavity. Meanwhile **R-62a** demonstrated strong affinity for both  $\text{Cs}^+$  and  $\text{Na}^+$ . The more polarizable  $\text{Cs}^+$  binding to **R-62a** was rationalized by the presence of nitrile groups which acted as  $\pi$ -donors. Furthermore, the high extractability and selectivity of **R-61b** and **R-62b** towards soft  $\text{Hg}^{2+}$  can be attributed to the soft nature of the sulphur atom in calix[4]-thia-crown. However, oxime derivatives **R-64** did not exhibit any selectivity even though all cations were extracted through cation- $\pi$  interactions with the  $\text{C}=\text{N}$  ligating groups.

Then, in 2018, Chen and Sun *et al.* employed acrylamido and propionamido substituents in calix[4]arene-crown-6-ether derivatives **R-65** to **R-67** for the selective extraction of  $\text{Cs}^+$  (Fig. 20).<sup>96</sup> In the LLE experiment, the distribution ratios of the receptors toward  $\text{Cs}^+$  were as follows: propionamido derivative (**R-67**) > acrylamido (**R-66**) > **R-65**. The deformation density of the Cs-complexes, as calculated from DFT using extended transition state coupled with natural orbitals for chemical valence (ETS-NOCV) analysis, indicated that the charge transfer occurred through the crown ether groups and the two rotated phenyl





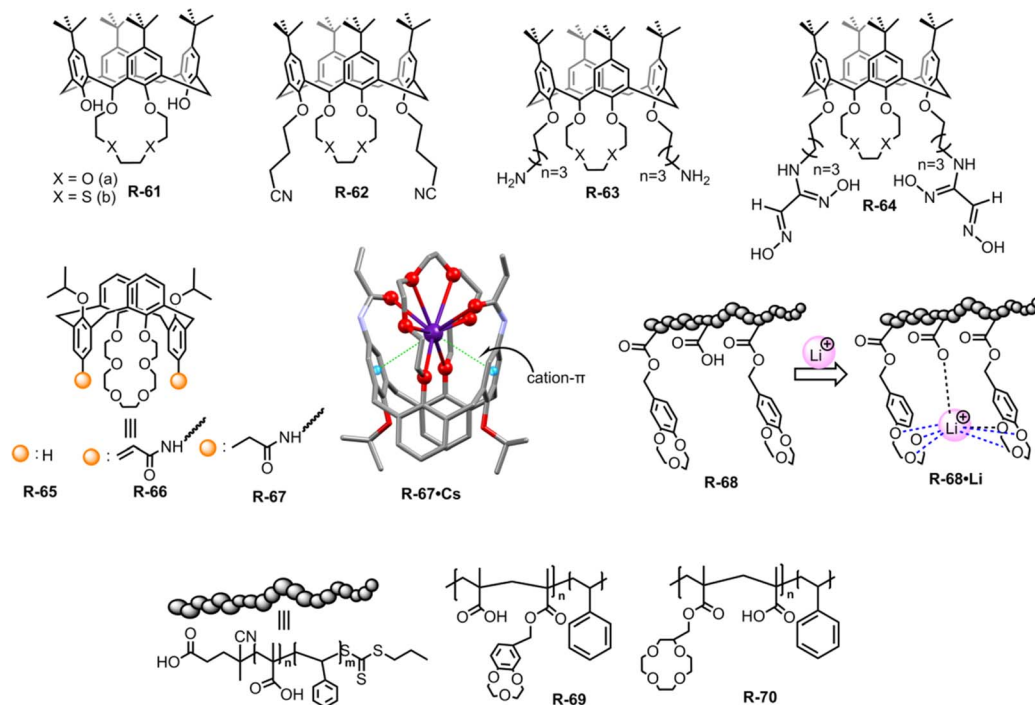


Fig. 20 Chemical structure of the receptors **R-61** to **R-70** and crystal structures of **R-67·Cs** (data from the Cambridge Crystallographic Data Centre [CCDC #1569925]<sup>96</sup>).

rings. Furthermore, the highest  $\text{Cs}^+$  affinity towards **R-66** and **R-67** was attributed to three intramolecular cooperative effects: (i) high affinity of the crown ether part for  $\text{Cs}^+$ , (ii) cation- $\pi$  interactions with the rotated phenyl rings, and (iii) interaction with the  $-\text{C}=\text{O}$  groups of the acrylamido or propionamido units. These triply cooperative effects were also supported by the solid-state structure. Based on the above consequence, the 1,3-alternate calix[4]arene crown-6 derivatives can improve the  $\text{Cs}^+$  extraction. Therefore, the aforementioned receptors elucidated that the well-organized arm of the calix[4]arene can provide harmony between the receptors and alkali metals which can further accelerate the ion-pair receptor design.

In recent decades, lithium ion ( $\text{Li}^+$ ) separation has become increasingly attractive due to its many application in our daily life, such as Li-ion batteries, medicines, catalysis, and in alloy industries.<sup>97–100</sup> However, selective extraction of  $\text{Li}^+$  is challenging over its other family members due to its larger hydration energy ( $-475 \text{ kJ mol}^{-1}$ ).<sup>38</sup> In this regard, just recently Abetz *et al.* developed a crown ether functionalized diblock copolymer **R-68** via RAFT polymerization by employing styrene and methacrylic acid as monomer units for the selective extraction of  $\text{Li}^+$  over other interfering alkali metal ions ( $\text{Na}^+$ ,  $\text{Cs}^+$ , and  $\text{K}^+$ ) (Fig. 20).<sup>101</sup> Moreover, in the LLE experiment, various crown ethers, including benzo-9-crown-3, benzo-12-crown-4, and benzo-15-crown-5, were employed along with the UV-responsive 2',4',5',7'-tetrabromoeosin ethyl ester salt of  $\text{Li}^+$ ,  $\text{Na}^+$  &  $\text{K}^+$ . The finding illustrated that the selective complexation of alkali metal ions depends on the cavity size of the crown ether and the stability of the complexes.<sup>102,103</sup> Hence, the polymer **R-68** based on benzo-9-crown-3 exhibited significant selectivity towards  $\text{Li}^+$  over  $\text{Na}^+$  and  $\text{K}^+$  attributed to the matching ionic size with the

cavity along with enthalpically driven sandwich-type complex formation. Furthermore, **R-68** displayed  $10^4$  times higher complex stability for  $\text{Li}^+$  compared to free benzo-9-crown-3. Importantly, the bound  $\text{Li}^+$  could easily be released from the polymer by raising the temperature. Hence, this polymer material holds promise for potential industrial applications in lithium recovery. Building upon the  $\text{Li}^+$  binding mechanism illustrated earlier, the same authors synthesized another two polymers **R-69** and **R-70** to improve the  $\text{Li}^+$  extraction from an aqueous medium. **R-69** exhibited a higher complexation constant ( $K$ ) ( $3.9 \times 10^{10} \text{ M}^{-1}$ ) compared to **R-70** ( $3.8 \times 10^7 \text{ M}^{-1}$ ) towards  $\text{Li}^+$  (Fig. 20).<sup>104</sup> Astonishingly, even in the presence of high concentrations of  $\text{Na}^+$  and  $\text{K}^+$ , **R-69** successfully extracted  $\text{Li}^+$  from seawater by forming a higher-order sandwich-type complex structure with  $\text{Li}^+$ .

Very recently, Weigand *et al.* investigated LLE by utilizing 4-phosphoryl pyrazolones **R-71** to **R-73** in the presence of various co-ligands (TOPO, TBPO and TBP) for the selective extraction of  $\text{Li}^+$  from the aqueous phase (Fig. 21).<sup>105</sup> In the presence of TOPO at pH 8.2, **R-73** exhibited maximum 78%  $\text{Li}^+$  extraction efficiency while it was 70 and 61% for **R-72** and **R-71** respectively. Surprisingly, in the absence of TOPO, the receptors demonstrated negligible (<5%)  $\text{Li}^+$  extraction efficiency. Hence, highly hydrophobic co-ligand TOPO played a pivotal role in extraction studies. Additionally, after  $\text{Li}^+$  extraction a noticeable visual colour change and chemical shifting of TOPO in the  $^{31}\text{P}$ -NMR spectrum suggested that the three  $\text{Li}^+$  ions were attached to the O-donor atom of TOPO forming a tetrahedral  $[\text{Li}_3\text{O}]$ -core which was the key factor for effective  $\text{Li}^+$  extraction. Thus, a new class of N, O, and P-donor-based receptors may aid in the investigation of coordination as well as extraction of s-block elements, mainly alkali metals, which are rarely observed.



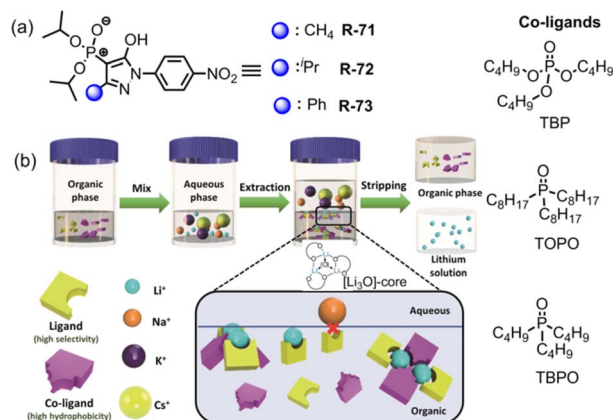


Fig. 21 (a) Chemical structure of the receptors **R-71** to **R-73**. (b) Schematic illustration of the  $\text{Li}^+$  extraction process with the presence of receptor and co-ligand. Reproduced with permission from ref. 105. Copyright 2022, Chemistry – A European Journal published by Wiley-VCH GmbH.

## 7. LLE of ion-pairs using ditopic receptors

In LLE, ion pair receptors play a crucial role in facilitating the transfer of cations along with anions from one phase to another. In this context, the ion pair receptor design usually involves incorporating hydrogen bond donor functional groups, as well as Lewis acidic sites or positively charged groups for the recognition of anions. For cations Lewis basic sites and  $\pi$ -electron moieties are integrated in the receptor. One of the first reports of an ion-pair receptor was made in 1991 by Reetz and co-workers.<sup>106</sup> Over the course of time, designing of such heteroditopic receptors was gradually developed. Several reviews have summarized this early progress on ion-pair binding.<sup>12,13,107–109</sup> Ion pair binding with different receptors can be categorized into three modes: (a) contact, (b) solvent-bridged and (c) host–guest separated ion pair (Fig. 22).

### 7.1. Metal halide salt extraction by ion-pair receptors

In 2018, Kim, Moyer, and Sessler *et al.* designed receptors **R-74** and **R-75** via an anion-selective calix[4]pyrrole unit strapped with a cationic domain hemispherand and phenanthroline unit respectively (Fig. 23).<sup>110</sup> From the crystal structure of the LiCl complex, the compact space within the receptor binds an alkali

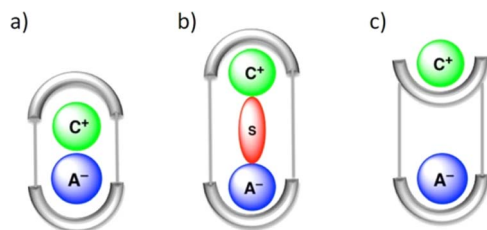


Fig. 22 Schematic representation of the binding modes for an ion pair receptor: (a) contact, (b) solvent-bridged, and (c) host–guest separated ion pair. (Reproduced from ref. 32. Copyright 2010 Royal Society of Chemistry.)

metal chloride salt through contact with a 1 : 1 stoichiometry, which maximises the coulombic interaction between the ion-pairs. Based on  $^1\text{H-NMR}$  studies, **R-74** was able to extract LiCl, NaCl, and KCl from  $\text{D}_2\text{O}$  to  $\text{C}_6\text{D}_5\text{NO}_2$  with selectivity order:  $\text{KCl} > \text{NaCl} > \text{LiCl}$ . The above selectivity can be described in terms of the hydration energies of the respective cations. In contrast to **R-74**, **R-75** showed  $\sim 100\%$  selectivity towards LiCl extraction from  $\text{D}_2\text{O}$  to  $\text{CDCl}_3$ . The latter observation reflected on the relatively small cavity size formed by the strapping unit in **R-75** which favoured the LiCl binding.

Later, Jang and co-workers contributed to the extraction of LiCl salts by synthesizing **R-76** (Fig. 23).<sup>111</sup> Inside the receptor, oligoethylene glycol was chosen as a Li-binding site while calix [4]pyrrole along with spacer triazole protons interacted with the counter halide ion. As indicated by the solid-state structure, **R-76** formed a 2 : 2 host–guest complex with LiCl. However, unlike the previous LiCl receptors, **R-76** exhibited a separated ion-pair binding. From the  $^1\text{H-NMR}$  in 1 : 10  $\text{CD}_3\text{OD}$  and  $\text{CD}_2\text{Cl}_2$  solvent, it was established that **R-76** selectively bound LiCl and LiBr. Furthermore, **R-76** was able to extract LiCl from water to an organic solvent ( $\text{CD}_2\text{Cl}_2$ ) in the presence of more than 80% saturated solution of LiCl. This extracted LiCl solution was further isolated as  $\text{Li}_2\text{CO}_3$  upon reacting with  $\text{CO}_2$  gas or solid  $\text{K}_2\text{CO}_3$ . Moreover, the amount of precipitated  $\text{Li}_2\text{CO}_3$  was calculated through acid–base titration using methyl orange as an indicator.



Fig. 23 Chemical structure of the receptors **R-74** to **R-83** and crystal structures of **R-74**·LiCl and **R-75**·LiCl (data from the Cambridge Crystallographic Data Centre [CCDC # 1821811 and 1821810 respectively]).<sup>110</sup>

To extract NaCl, Romanski and co-workers prepared a heteroditopic receptor **R-77** by integrating a 15-crown-5 moiety and anion-selective squaramide unit (Fig. 23).<sup>112</sup> This receptor cooperatively interacted with  $\text{Cl}^-$  in the presence of  $\text{Na}^+$  as directed by the  $\text{Cl}^-$  binding constant of the cation-free ( $1.15 \times 10^5 \text{ M}^{-1}$ ) and cation-bound receptor ( $1.97 \times 10^5 \text{ M}^{-1}$ ) derived from UV studies in  $\text{CH}_3\text{CN}$ . This enhancement of the association constant was rationalized by the increasing acidity of the squaramide protons induced by cation binding. Under LLE conditions, NaCl was transferred by the host from water to the  $\text{C}_6\text{D}_5\text{NO}_2$  solvent, as indicated by the large chemical shifts ( $\Delta\delta = 0.72$  and  $0.79$  ppm) of the two squaramide NH-protons. Additionally, by back-extracting the NaCl into the water, **R-77** could also be freed easily. However, receptors **R-78** and **R-79** failed to extract NaCl, which signified the lower acidity of urea-NHs over squaramide protons and the superiority of heteroditopic receptors for ion-pair binding, respectively.

In 2020, the extraction of inorganic salts was reported by Sindelar *et al.* with aza-crown ether functionalized bambus[6]uril receptors **R-80** and **R-81** (Fig. 23).<sup>113</sup> The typical anion receptor bambusurils effectively bind anions into the cavity with 12 methine- $\text{H} \cdots \text{A}^-$  hydrogen bond interactions. Phase separation between the  $\text{CHCl}_3$  solution of receptors and the aqueous solution of inorganic salts allowed the extraction of inorganic salts including NaCl to the receiving organic phase. Both the methine and crown- $\text{CH}_2$  protons were shifted in  $^1\text{H-NMR}$  implying a successful extraction process, whereas the methine proton integration allowed the extraction efficiency to be determined. For both the receptors, the higher extraction ability for MI and MBr salts ( $\text{M} = \text{Li}, \text{Na}, \text{K}$ ) was justified by the larger binding affinities of these anions toward bambusuril, while for MCl salt extraction depended on the counter cation and crown ether size of the receptor. Thus, **R-81** extracted  $\sim 100\%$  NaBr and NaI from water, while only 74% efficiency was noted for NaCl.

In later studies, the same group reported two bambus[6]uril derivatives **R-82** and **R-83**, and demonstrated their anion extraction and transport ability (Fig. 23).<sup>114</sup> Herein, they introduced an electron withdrawing as well as lipophilic substituent into the receptor to improve interaction with small hydrated anions. Both receptors were capable of quantitatively extracting the tetrabutylammonium salts of  $\text{Cl}^-$ ,  $\text{NO}_3^-$ , and  $\text{H}_2\text{PO}_4^-$  from water to the organic nitrobenzene phase. However, among the inorganic salts, **R-82** could only extract  $\text{NaNO}_3$  with 68% efficiency due to the receptor having a strong affinity towards smaller  $\text{NO}_3^-$ . In contrast, for **R-83**, inorganic salt extraction depended on the cavity size of the aza-crown ether. Thus, a preferable KCl (41%) extraction over NaCl (36%) was observed, whereas, in the case of  $\text{NaNO}_3$  salt, **R-83** showed quantitative extraction. These two studies established the efficacy of bambusuril-based receptors for extraction. Moreover, the incorporation of squaramide and calix[4]pyrrole units in the receptors also played a crucial role in binding hard-to-capture ion pairs.

The selective separation of highly hydrated KF and KCl salts from the water medium is of fundamental importance in chemistry. In this context, our group for the first time reported solvent extraction of KF from water to  $\text{CHCl}_3$  using a 'dual host'

strategy. Besides ditopic receptors, ion pair binding through a dual host system (binary mixture of two receptors) has also proved to be promising. This dual host strategy could be more versatile and economical instead of designing complex receptors for salt extraction application. In our approach, 18-crown-6 (**R-84a**) and a tripodal amide receptor **R-84b** were used as dual hosts. The later tripodal receptor effectively bound halide through 3 acidic 'NH' protons (Fig. 24).<sup>115</sup> The crystal structure clearly revealed the formation of a 1D coordination polymer with the KF guest where  $\text{K}^+$  and  $\text{F}^-$  were encapsulated in the respective domains. Such encapsulation was also confirmed from the downfield chemical shift of the NH protons in the  $^1\text{H-NMR}$  in  $\text{CDCl}_3$ . An extraction enhancement of anions ( $\text{F}^-$  and  $\text{Cl}^-$ ) with the  $\text{K}^+$ -bound receptor defined the dual host synergistic extraction of KF and KCl. At pH  $\sim 6.0$ , 48% and 44% extraction efficiency were observed for KF and KCl respectively.

Later, Sessler and co-workers reported multitopic receptor **R-85** for KF extraction. Anion selective calix[4]pyrrole and cation selective crown-linked calix[4]arene were connected through ethylene glycol spacers, thus forming multiple recognition zones inside the receptor (Fig. 24).<sup>116</sup> An  $^1\text{H-NMR}$  study in a 1 : 9  $\text{CD}_3\text{OD}/\text{CDCl}_3$  solvent mixture revealed that **R-85** was capable of binding both KF and CsF salts. However, distinct binding modes and complexation processes were observed for each. In the mentioned solvent system, a relatively stronger binding of  $\text{K}^+$  ( $6.5 \times 10^6 \text{ M}^{-1}$ ) to the upper crown pocket was observed compared to  $\text{Cs}^+$  ( $3.3 \times 10^4 \text{ M}^{-1}$ ). This robust binding led to the selective extraction of KF salt from water to the nitrobenzene phase through the formation of the 1 : 1 [**R-85**·KF] complex. KF

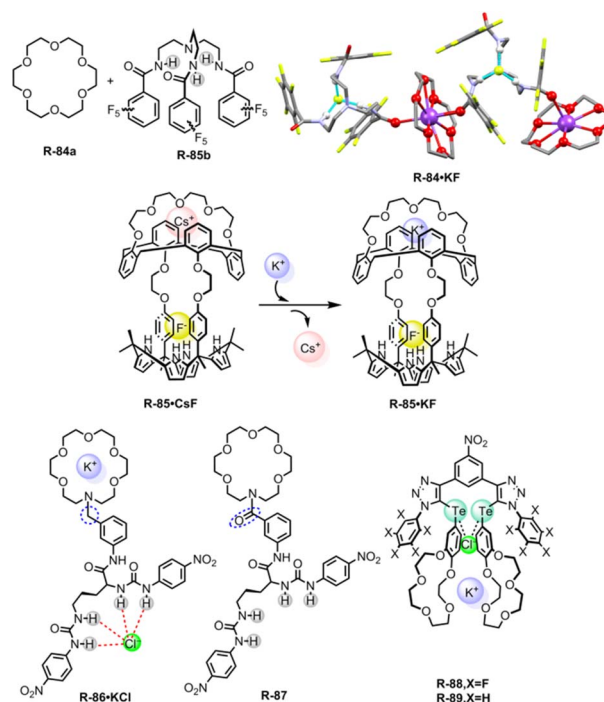


Fig. 24 Chemical structure of the receptors **R-84** to **R-89** with ion-pair binding and crystal structures of **R-84**·KF (data from the Cambridge Crystallographic Data Centre [CCDC # 732760]).<sup>115</sup>





extraction was also well supported by the large chemical shift of the calix -NH protons ( $\Delta\delta = 5.1$  ppm) of the extracted organic phase. In contrast, CsF could not significantly alter the proton signals, indicating lower efficiency of the receptor under the LLE conditions. Additionally, the strong binding of  $K^+$  to the upper crown pocket displaced the weakly bound  $Cs^+$  from the receptor through the 'cation metathesis' process. Thus, **R-85** demonstrated a new idea of recyclable receptor designing, where cation metathesis could play a significant role.

A notable study on the cooperative effects during ion-pair binding was performed by Piątek and co-workers. In 2017, they constructed two ion-pair receptors, **R-86** and **R-87**, *via* linking aza-18-crown-6 with urea-functionalized amino acid L-ornithine (Fig. 24).<sup>117</sup> The only difference between **R-86** and **R-87** was the spacer unit (benzyl *vs.* benzoyl) which played a vital role in anion recognition. In **R-87**, the presence of a less conformationally flexible amide spacer near the cation domain caused less cooperative ion-pair binding. In contrast, the flexible benzyl version **R-86** showed significant cooperation during ion-pair binding specially for KCl and  $NH_4Cl$ . UV-Vis spectroscopic analysis in  $CH_3CN$  demonstrated almost 8 times higher  $Cl^-$  binding ability to the **R-86** over **R-87** in the presence of the  $K^+$  ion with binding constant values of  $3.7 \times 10^5$  and  $4.4 \times 10^4 M^{-1}$  respectively. The interaction mechanism was established by  $^1H$ -NMR studies in  $CD_3CN$  which revealed anion binding involving all the urea protons and cation encapsulation to the crown ether moiety. Furthermore, **R-86** showed efficient extraction capacity for KCl (97%) as well as  $NH_4Cl$  (93%) under LLE conditions while **R-87** failed to extract the same from  $H_2O$  to  $CHCl_3$ .

In parallel to hydrogen bonding, Beer and his colleagues recently synthesized a heteroditopic receptor **R-88** by employing  $\sigma$ -hole-based chalcogen bonding (ChB) interaction (Fig. 24).<sup>27</sup> Binding of a cation in the crown moiety induced the formation of strongly polarised  $\sigma$ -holes on Te-atoms. Electron-withdrawing pentafluorobenzene substituents were also involved in such polarization. NMR titration in 1:1  $CDCl_3/CD_3CN$  in the presence of equimolar  $KPF_6$  exhibited relatively higher association constants for  $Cl^-$  over other common anions. Under LLE conditions, almost 71% KCl was extracted from  $D_2O$  to  $CDCl_3$  when the KCl concentration was 4 M. Moreover, nonfluorinated receptor **R-89** failed to extract KCl under identical conditions, indicating a lower effect of electron polarization on chalcogen bonding. Therefore, appropriately designed ChB receptors are able to bind a harder Lewis base through a polarized  $\sigma$ -hole, offering a potential alternative for selective salt extraction from water.

It has been found that the supramolecular self-assembly procedure is efficient for the recognition and extraction of ion pairs. In these cases, a properly designed molecule interacts with the guests *via* non-covalent interactions and thereby aggregates to form various supramolecular self-assembly structures (such as micelles, vesicles).<sup>118</sup>

In 2017, Sessler and colleagues designed a receptor **R-90**, in which the calix[4]pyrrole subunit and long-tailed anthracene moiety were connected by a triazole spacer (Fig. 25).<sup>119</sup> This long-tailed host undergoes self-assembly in an aqueous



Fig. 25 (a) Chemical structure of the receptors **R-90** and **R-91**. (b) Self-assembly driven micelle formation at the interface by **R-91**. (Reproduced with permission from ref. 120. Copyright 2018, ACS Publication.)

medium upon binding  $Fe^{2+}$  and  $F^-$  into the respective recognition sites, forming cross-linkable micelles at the interface. The change in polarity upon guest binding resulted in the formation of micelles, as confirmed by microscopic analyses such as scanning electron microscopy (SEM) and transmission electron microscopy (TEM). Moreover, by forming such assemblies, the receptor **R-90** demonstrated notable efficiency in extracting  $FeF_2$ , as evidenced by approximately 75% extraction yield, as indicated by  $^{19}F$ -NMR.

In a later report, the same group found a separation method for CsF salt under LLE conditions *via* a diblock copolymer receptor **R-91** (Fig. 25).<sup>120</sup> In  $CH_2Cl_2$  solvent, receptor **R-91** formed reversed micelles *via* aggregation (Fig. 25b) after binding to  $Cs^+$  and  $F^-$ , which was confirmed by TEM, dynamic light scattering (DLS), and energy-dispersive X-ray analysis. Solvent extraction of CsF salt from water to  $CH_2Cl_2$  unequivocally indicated the self-assembly process to be a good driving force for solvent extraction.

## 7.2. Metal oxo-anion salt extraction by ion-pair receptors

Sessler and his group prepared **R-92** by connecting calix[4]pyrrole with the cationic domain hemispherand unit. This tri-topic receptor can serve as an extractant for both MX and  $M_2X$  type metal salts. In 2016, this receptor was utilized for the recognition of exceptionally hydrated lithium salts (Fig. 26).<sup>121</sup> **R-92** demonstrated the capability to bind various Li salts, including LiCl, LiBr, LiI,  $LiNO_2$ , and  $LiNO_3$ , as confirmed by crystal structures.  $^1H$ -NMR analysis in 1:9 (v/v)  $CD_3OD/CD_2Cl_2$



revealed a preferential binding of  $\text{Li}^+$  salt over  $\text{Na}^+$ ,  $\text{K}^+$ , and  $\text{Rb}^+$  metals salts. Moreover, **R-92** selectively extracted  $\text{LiNO}_2$  over  $\text{NaNO}_2$  and  $\text{KNO}_2$  from water to the organic phase, which appeared to be significant for corrosion inhibition in the construction industry.

Later, **R-92** was also proved to bind both MX type Cs-salts, namely, halides and hydroxide as well as  $\text{M}_2\text{X}$  type  $\text{Cs}_2\text{CO}_3$  (Fig. 26).<sup>122</sup> For  $\text{Cs}_2\text{CO}_3$ , one  $\text{Cs}^+$  was bound to the cavity offered by the hemispherand unit, while the other  $\text{Cs}^+$  was bound 'in the cup' formed by the combination of pyrrolic units to finally make a 1 : 1 **R-92**· $\text{Cs}_2\text{CO}_3$  complex. From  $^1\text{H-NMR}$  and ICP-MS investigations, it was revealed that **R-92** can extract  $\text{Cs}_2\text{CO}_3$  and  $\text{CsOH}$  over  $\text{CsX}$  ( $\text{X} = \text{halide}$ ) salts from the highly basic aqueous phase to the organic  $\text{CDCl}_3$  phase. This result suggested that **R-92** may overcome the large hydration enthalpies of the anions  $\text{OH}^-$  ( $-430 \text{ kJ mol}^{-1}$ ) and  $\text{CO}_3^{2-}$  ( $-1315 \text{ kJ mol}^{-1}$ ). Furthermore, the U-tube transport experiment was also carried out using **R-92**, to confirm the transport of  $\text{CsOH}$  through the organic  $\text{CHCl}_3$  layer.

An early example of selective Cs salt extraction was reported in 2010 by the same group. A co-polymeric receptor, **R-93**, comprising benzocrown-6-calix[4]arene as the core recognition unit was found to be selective towards  $\text{Cs}^+$  (Fig. 26).<sup>123</sup>  $^1\text{H-NMR}$

revealed that **R-93** was a selective extractor for  $\text{CsNO}_3$  over other Cs-salts like  $\text{CsX}$  ( $\text{X} = \text{halide}$ ),  $\text{CsSO}_4$  and other nitrate salts like  $\text{KNO}_3$  and  $\text{NaNO}_3$ . Thus, a  $\text{CD}_2\text{Cl}_2$  solution of **R-93** extracted  $\text{CsNO}_3$  from an aqueous solution in the presence of the above-mentioned salts. Additional evidence of  $\text{CsNO}_3$  extraction was obtained from ICP-MS studies which showed almost 60%  $\text{Cs}^+$  complexation with respect to the receptor. Furthermore, the extracted host-guest complex was isolated by adding cold hexane resulting in the formation of a precipitate, which gave 10% more mass than the free receptor indicating guest binding.

Salt extraction by colorimetric receptors provides an additional advantage because they can induce rapid detection, leading to a visual colour change in the organic phase. Specifically, this array provides an attractive alternative compared to other existing techniques due to its efficiency and lack of complexity, making it less time-consuming and presumptive. In this regard, Sessler and co-workers synthesized receptor **R-94** by connecting a chromophore (3-(dicyanomethylidene) indan-1-one) functionalised calix[4]pyrrole with calix[4]arene through an ethylene glycol spacer (Fig. 26).<sup>124</sup> In 1 : 10  $\text{CH}_3\text{OH}/\text{CHCl}_3$ , UV-Vis spectroscopic analysis of **R-94** indicated selective interaction with Cs-salts including  $\text{CsF}$ ,  $\text{CsCl}$  and  $\text{CsNO}_3$  with the formation of a 1 : 1 complex. Furthermore, the recognition ability of **R-94** was observed only in the presence of  $\text{CsX}$  ( $\text{X} = \text{F}, \text{Cl}, \text{Br}, \text{NO}_3, \text{ClO}_4$ ) salts rather than individual  $\text{Cs}^+$  or  $\text{X}^-$  ions. Therefore, **R-94** acted as a chemical AND logic gate for ion-pair binding.  $^1\text{H-NMR}$  spectral changes of  $-\text{NH}$  protons in **R-94** supported the selective extraction of  $\text{CsNO}_3$  from  $\text{D}_2\text{O}$  to  $\text{C}_6\text{D}_5\text{NO}_2$ . Such ion-pair binding to the receptor caused an alteration of the electronic environment within the chromophore unit leading to a visual colour change of the organic solution.

Another example of  $\text{CsNO}_3$  salt extraction from the aqueous to organic nitrobenzene phase was reported with the previously mentioned receptor **R-85** (Fig. 24).<sup>125</sup> In this case,  $\text{CsNO}_3$  complexed with the receptor in a contact mode, where  $\text{Cs}^+$  bound to the defined cavity of the ethylene glycol spacer along with nitrate binding to the calix-pyrrole unit. However, the strong affinity of the upper 1,3-alternate calix-crown system towards  $\text{K}^+$  initiated cation metathesis by replacing  $\text{Cs}^+$  with  $\text{K}^+$  within the receptor. Thus, addition of a  $\text{KClO}_4$  solution in 1 : 9  $\text{CD}_3\text{OD}/\text{CDCl}_3$  to a  $\text{CsNO}_3$  complex in the same solvent leads to the formation of  $[\text{R-85} \cdot \text{K}^+]\text{ClO}_4^-$  as a white precipitate. As indicated by  $^1\text{H-NMR}$ , **R-85** could extract  $\text{CsNO}_3$  from water to nitrobenzene even in the presence of competing  $\text{NaNO}_3$ . Moreover, this extracted  $\text{CsNO}_3$  could be released back to the aqueous phase by adding an aq.  $\text{KClO}_4$  solution. Ultimately the free receptor could be recovered after  $\text{H}_2\text{O}/\text{CHCl}_3$  contact (Fig. 27). Thus, as mentioned earlier, the metathesis process within the ion-pair receptor provided the preliminary idea of the recyclable receptor design as well as the on-off switching mechanism of extraction.

In 2012, Romanski and Piątek prepared heteroditopic monomeric receptor **R-95** and its polymer **R-96** using an L-ornithine scaffold (Fig. 28).<sup>126</sup> Solution phase studies in  $\text{CH}_3\text{CN}$  indicated effective binding of  $\text{Na}^+$  into the aza-crown moiety which in turn enhanced the nitrate ( $\text{NO}_3^-$ ) binding to the



Fig. 26 Chemical structure of the receptors **R-92** to **R-94** (data from the Cambridge Crystallographic Data Centre [CCDC # 1483286, 1483283, 1549914].<sup>121,122</sup>) and visible colour change observed for **R-94** during the LLE experiment. (Reproduced with permission from ref. 124. Copyright 2016, ACS Publication.)



Fig. 27 Schematic illustration of the two-phase extraction through the cation metathesis process by **R-85**. (Reprinted from ref. 125. Copyright 2012, ACS Publication.)

thiourea section. However, negative cooperativity was observed for  $\text{Cl}^-$  and  $\text{CH}_3\text{COO}^-$  in the presence of  $\text{Na}^+$  indicating ion-pairing outside the receptor. Therefore, solvent extraction of  $\text{NaNO}_3$  from water to  $\text{CHCl}_3$  was performed. However, extraction of nitrate with **R-95** appeared negligible, while the polymeric receptor **R-96** could accomplish the same extraction with 32% efficiency as determined by the colorimetric nitrite–nitrate technique. Additionally, co-extraction of  $\text{Na}^+$  was confirmed by atomic emission spectroscopy which measured  $\sim 44\%$  sodium content by mass of the organic phase after the extraction. Furthermore, analogous extraction experiments for  $\text{NaCl}$  by **R-96** resulted in 19% sodium extraction. This report emphasized that a properly designed polymeric system could be a better salt extractant than its monomeric analogue.

The same group had synthesized a series of heteroditopic receptors **R-97** to **R-101** and studied their cooperative ion-pair

interaction with respect to the geometrical as well as electronic environment of the receptors (Fig. 28).<sup>127</sup> For **R-97** to **R-99**, control  $^1\text{H}$ -NMR in  $\text{CD}_3\text{CN}$  established the fact that the co-bound  $\text{Na}^+$  enhanced the nitrite ( $\text{NO}_2^-$ ) binding rather than the non-coordinating  $\text{TBA}^+$  cation that indicates cooperative interaction for the former case. The urea oxygen atom upon coordinating with the bound  $\text{Na}^+$  increased the acidity of the urea protons resulting in such positive cooperativity. In addition to urea NH, the functionalised amide  $-\text{NH}$  substituent interacted with the anion through a hydrogen bond. Interestingly, **R-99** showed the highest cooperativity compared to other receptors including **R-101**. This highlighted a stronger effect of the favourably positioned electron-withdrawing  $-\text{CF}_3$  group on polarizing NH protons for anion recognition. In fact, in **R-101** the exceptionally strong influence of  $-\text{SO}_2\text{CF}_3$  resulted in the subsequent deprotonation of the urea protons upon binding with the anion. However, in the LLE experiment, **R-99** could extract  $\text{NaNO}_2$  to the receiving organic phase with 3.1% efficiency as proved by NMR analysis.

In 2018, the same group constructed receptor **R-102** based on an *L*-valine platform (Fig. 28).<sup>128</sup> Unlike *L*-ornithine amino acid, *L*-valine lacks the extra anion binding amine group. However, in **R-102**, acid functionalised 18-crown-6 strongly bound cations and enhanced the anion binding ability. Thus, in the presence of  $\text{K}^+$ , the anion association constant for  $\text{CH}_3\text{COO}^-$  binding exceeded  $10^7$  orders as obtained from UV-Vis studies in  $\text{CH}_3\text{CN}$ . Discernible chemical shifts of the NH protons ( $\sim 2$  ppm) and crown  $-\text{OCH}_2$  protons indicated  $\sim 100\%$   $\text{CH}_3\text{COOK}$  salt extraction from water to the  $\text{CDCl}_3$  phase.

In 2021, they prepared a series of receptors **R-103** to **R-107** by changing the gap between core cation and anion binding groups (Fig. 28).<sup>129</sup> The amide  $-\text{NH}$  proton, in addition to urea protons, played a significant role in  $\text{CH}_3\text{COO}^-$  binding. In **R-104**

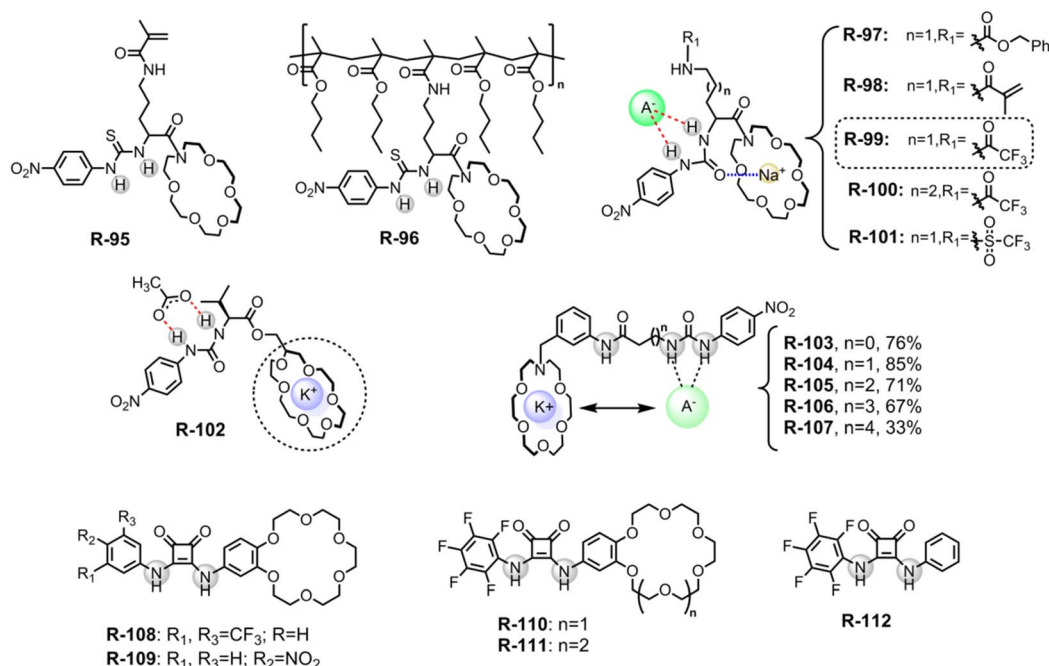


Fig. 28 Chemical structure of the receptors **R-95** to **R-112**.



and **R-105**, the increased conformational flexibility enabled greater involvement of the amide-NH proton in anion binding. Meanwhile, in **R-106** and **R-107** less involvement of amide -NH protons for anion binding was justified in terms of the larger gap between the urea group and amide -NH protons. In **R-103**, conformational rigidity restricted the amide -NH protons for anion binding. In accordance with the design features of the receptors, the increasing distance between the cation and anion binding group allows a more flexible and lipophilic host resulting in a more polar host-guest complex formation at the interface ultimately reducing the extraction capability. However, due to less conformational freedom, the most rigid receptor **R-103** (76%) was less efficient than **R-104** (85%) in the extraction of  $\text{CH}_3\text{COOK}$  salt.

The critical feature of receptors **R-95** to **R-107** is the urea or thiourea connectivity involved in anion recognition. Romański and co-workers, instead, use squaramide as it provides more polarised protons compared to urea or thiourea groups. The increased aromaticity of the squaramide ring following anion complexation emphasises the defined polarisation of its protons. Accordingly, in 2019, heteroditopic receptors **R-108** and **R-109** were synthesized. Binding of  $\text{K}^+$  in the crown moiety which induced  $\text{SO}_4^{2-}$  binding with the squaramide protons eventually overcame the dominating hydration energy for  $\text{SO}_4^{2-}$  recognition in aqueous solution (Fig. 28).<sup>130</sup> The solid-state structures revealed 4:1 receptor- $\text{SO}_4^{2-}$  complex formation through 8 hydrogen bonds, while a 1:1 stoichiometry was observed for  $\text{KNO}_3$ . Such larger stoichiometry resulted in receptor- $\text{SO}_4^{2-}$  assembly which was confirmed by a reduction of the diffusion coefficient in DOSY NMR. Furthermore, such strong interaction associated with the receptor- $\text{SO}_4^{2-}$  complex preferentially extracted  $\text{K}_2\text{SO}_4$  from the aqueous to the  $\text{CDCl}_3$  phase even in the presence of  $\text{KNO}_3$ . Thus, from the solution containing 10 times higher  $\text{KNO}_3$ , the receptor extracted  $\text{K}_2\text{SO}_4$  with 64% efficiency.

Interestingly, receptor **R-109** acted as a colorimetric sensor for  $\text{SO}_4^{2-}$  extraction which was described in terms of -NH deprotonation of the extremely acidic squaramide.

Similarly, large stoichiometry (4:1) was observed for host- $\text{SO}_4^{2-}$  binding with receptors **R-110** to **R-112**. Among them, **R-111** showed better cooperativity for ion-pair binding as indicated by the initial UV-Vis studies in  $\text{CH}_3\text{CN}$ .<sup>131</sup> This could be attributed to the interplay of favourable allosteric and electrostatic factors between the receptor and the ion-pair. **R-112**, without the cationic domain, was less efficient for anion recognition (Fig. 28). For **R-111**, the formation of a similar host- $\text{K}_2\text{SO}_4$  core-shell assembly was confirmed and assumed to be the functional driving force for the selective extraction of  $\text{K}_2\text{SO}_4$  to the  $\text{CHCl}_3$  phase. Atomic emission spectroscopy measured potassium content of 51%, 58%, 61%, and 90% by mass of the organic phase after extraction from 0.5 M aqueous solutions of KCl, KBr, KI, and  $\text{K}_2\text{SO}_4$ , respectively. Moreover, the control U-tube experiment established the relatively higher transportability of  $\text{KNO}_3$  and KCl salts by the **R-111** over  $\text{K}_2\text{SO}_4$ , representing stronger receptor- $\text{K}_2\text{SO}_4$  complex formation.

## 8. Outlook and conclusions

Supramolecular non-covalent interactions have been used for LLE of anions as well as cations. Over the past few decades, this field of chemistry has evolved from almost nothing into a rapidly maturing field of research. In this perspective, we illustrate the progress of LLE by highlighting, in particular, receptor engineering for selective guest binding following the supramolecular approach. Moreover, the breadth of practical applications of this extraction principle in water treatment, environmental cleanup, and corrosion inhibition is also addressed. In these extraction processes, success is accomplished by leveraging relatively weak interactions. Separating ionic species, of great importance for environmental concern, is often fraught with difficulties due to their high hydration energies and this emphasizes the need for appropriate receptor design with sufficient binding sources. In this regard, we categorized the perspective based on an ionic guest and covered the liquid-liquid extractants for halides, oxo-anions, cations, and ion-pairs. This may pave the way for designing more receptors that can overcome the Hofmeister bias to extract more hydrated ions and cooperatively bind the guests to ensure ion-pair extraction. Besides, we envisioned that receptors having XB and ChB donor motifs instead of an HB domain could be a better option for LLE of selective anions due to their directional and hydrophobic character. Soluble polymeric receptor designing could be another fruitful way to conduct LLE which is also limited in number. Additionally, there is a need to investigate supramolecular self-assembly-driven LLE processes for the potential separation of highly solvated anions. This approach could also enhance the reusability of the receptors. In order to keep pace with the ever-expanding industrial demands specifically in the petrochemical, pharmaceutical, and metallurgical industry sectors, extensive research should be committed to the development of receptors capable of separating and purifying industrial guests *via* LLE. Nevertheless, this technique provides an economical and energy-efficient process for purifying wastewater, making it a promising and effective alternative in industry.

In summary, the current instances of supramolecular receptors in the context of LLE presented in this perspective will catch the attention of chemists, biochemists, environmental scientists, and materials and metallurgy scientists along with the chemical and pharmaceutical industries. Furthermore, they will also attract the interest of undergraduate and graduate students who are interested in application-oriented research related to industrial and environmental issues.

## Data availability

X-ray crystallography structural files are available free of charge from the CCDC *via* <https://www.ccdc.cam.ac.uk/>.

## Author contributions

S. P., A. S. M. I., I. G. and P. G. conceived and collaboratively drafted the manuscript.



## Conflicts of interest

There are no conflicts to declare.

## Acknowledgements

This work was financially supported by the Science and Engineering Research Board (SERB; CRG/2019/002236; PDF/2019/000353) and J. C. Bose National Fellowship (JCB/2021/000032). A. S. M. I. acknowledged SERB for NPDP. S. P. and I. G. thanks CSIR and Inspire, respectively for fellowship.

## Notes and references

- 1 A. J. Savyasachi, O. Kotova, S. Shanmugaraju, S. J. Bradberry, G. M. Ó'Máille and T. Gunnlaugsson, *Chem*, 2017, **3**, 764–811.
- 2 J. W. Steed and J. L. Atwood, *Supramolecular Chemistry*, John Wiley & Sons, 2nd edn, 2009.
- 3 J.-M. Lehn, *Angew. Chem., Int. Ed.*, 1988, **27**, 89–112.
- 4 N. Busschaert, C. Caltagirone, W. V. Rossom and P. A. Gale, *Chem. Rev.*, 2015, **115**, 8038–8155.
- 5 E. D. Doidge, I. Carson, P. A. Tasker, R. J. Ellis, C. A. Morrison and J. B. Love, *Angew. Chem., Int. Ed.*, 2016, **55**, 12436–12439.
- 6 E. D. Doidge, L. M. M. Kinsman, Y. Ji, I. Carson, A. J. Duffy, I. A. Kordas, E. Shao, P. A. Tasker, B. T. Ngwenya, C. A. Morrison and J. B. Love, *ACS Sustainable Chem. Eng.*, 2019, **7**, 15019–15029.
- 7 M. Sharma, P. Sharma and J. N. Kim, *RSC Adv.*, 2013, **3**, 10103–10126.
- 8 G. Zhang, Y. Ding, A. Hashem, A. Fakim and N. M. Khashab, *Cell Rep. Phys. Sci.*, 2021, **2**, 100470.
- 9 X. Zhao, J. Liu, J. Fan, H. Chao and X. Peng, *Chem. Soc. Rev.*, 2021, **50**, 4185–4219.
- 10 R. Ghosh, T. K. Ghosh, S. Pramanik, A. S. M. Islam and P. Ghosh, *ACS Appl. Mater. Interfaces*, 2023, **15**, 25184–25192.
- 11 R. Ghosh, T. K. Ghosh and P. Ghosh, *Dalton Trans.*, 2020, **49**, 3093–3097.
- 12 Q. He, G. I. Vargas-Zuniga, S. H. Kim, S. K. Kim and J. L. Sessler, *Chem. Rev.*, 2019, **119**, 9753–9835.
- 13 A. Li, H. Zhai, J. Li and Q. He, *Chem. Lett.*, 2020, **49**, 1125–1135.
- 14 Q. Zhang, Y. Zhou, M. Ahmed, N. M. Khashab, W. Han, H. Wang, Z. A. Page and J. L. Sessler, *J. Mater. Chem. A*, 2022, **10**, 15297–15308.
- 15 G. I. Vargas-Zúñiga, H. Qing and J. L. Sessler, *Ion Exchange and Solvent Extraction*, CRC Press, 2019, vol. 23, pp. 45–82.
- 16 G. I. Vargas-Zúñiga and J. L. Sessler, *Comprehensive Supramolecular Chemistry II*, ed. Atwood, J. L., Elsevier, Oxford, U.K., 2017, pp. 161–189.
- 17 B. A. Moyer and P. V. Bonnesen, Physical Factors in Anion Separations, in *The Supramolecular Chemistry of Anions*, ed. A. Bianchi, K. Bowman-James and E. García-España, VCH, Weinheim, Germany, 1997, ch. 1, pp. 1–44.
- 18 K. Gloe, K. Gloe, M. Wenzel, L. F. Lindoy and F. Li, *Supramolecular chemistry in solvent extraction: toward highly selective extractants and a better understanding of phase-transfer phenomena*, CRC, U.S.A., 2013.
- 19 S. Kubik, *Chem. Soc. Rev.*, 2010, **39**, 3648–3663.
- 20 I. A. Rather, S. A. Wagay and R. Ali, *Coord. Chem. Rev.*, 2020, **415**, 213327.
- 21 L. J. Chen, S. N. Berry, X. Wu, E. N. W. Howe and P. A. Gale, *Chem*, 2020, **6**, 61–141.
- 22 M. Wenzel, J. J. Weigand and J. Inclusion Phenom, *Macrocyclic Chem.*, 2017, **89**, 247–251.
- 23 J. Rydberg, *Solvent extraction principles and practice, revised and expanded*, CRC press, 2nd edn, 2004.
- 24 V. S. Kislík, *Solvent extraction: classical and novel approaches*, Elsevier, 2011.
- 25 B. Schnell, R. Schurhammer and G. Wipff, *J. Phys. Chem. B*, 2004, **108**, 2285–2294.
- 26 Y. Liu, W. Zhao, C. H. Chen and A. H. Flood, *Science*, 2019, **365**, 159–161.
- 27 A. Docker, I. Marques, H. Kuhn, Z. Zhang, V. Félix and P. D. Beer, *J. Am. Chem. Soc.*, 2022, **144**(32), 14778–14789.
- 28 B. Schuur, B. J. V. Verkuil, A. J. Minnaard, J. G. De Vries, H. J. Heeres and B. L. Feringa, *Org. Biomol. Chem.*, 2011, **9**, 36–51.
- 29 X. M. Wu and W. J. Wu, *Food Chem.*, 2012, **134**, 597–601.
- 30 X. Wu, A. M. Gilchrist and P. A. Gale, *Chem*, 2020, **6**, 1296–1309.
- 31 N. H. Evans and P. D. Beer, *Angew. Chem., Int. Ed.*, 2014, **53**, 11716–11754.
- 32 S. K. Kim and J. L. Sessler, *Chem. Soc. Rev.*, 2010, **39**, 3784–3809.
- 33 G. W. Gokel, W. M. Leevy and M. E. Weber, *Chem. Rev.*, 2004, **104**, 2723–2750.
- 34 X. Zhang and C. Wang, *Chem. Soc. Rev.*, 2011, **40**, 94–101.
- 35 C. Wang, Z. Wang and X. Zhang, *Acc. Chem. Res.*, 2012, **45**, 608–618.
- 36 U. V. Gunten, *Water Res.*, 2003, **37**, 1469–1487.
- 37 N. R. Johnston and S. A. Strobel, *Arch. Toxicol.*, 2020, **94**, 1051.
- 38 Y. Marcus, *J. Chem. Soc., Faraday Trans.*, 1991, **87**, 2995–2999.
- 39 C. W. Chiu and F. P. Gabbaï, *J. Am. Chem. Soc.*, 2006, **128**, 14248–14249.
- 40 P. Das, A. K. Mandal, M. K. Kesharwani, E. Suresh, B. Ganguly and A. Das, *Chem. Commun.*, 2011, **47**, 7398–7400.
- 41 P. R. Brotherhood and A. P. Davis, *Chem. Soc. Rev.*, 2010, **39**, 3633–3647.
- 42 J. P. Clare, A. J. Ayling, J. B. Joos, A. L. Sisson, G. Magro, M. N. Pérez-Payán, T. N. Lambert, R. Shukla, B. D. Smith and A. P. Davis, *J. Am. Chem. Soc.*, 2005, **127**, 10739–10746.
- 43 S. J. Edwards, H. Valkenier, N. Busschaert, P. A. Gale and A. P. Davis, *Angew. Chem.*, 2015, **127**, 4675–4679.
- 44 V. Amendola, G. Bergamaschi, M. Boiocchi, L. Fabbri and M. Milani, *Chem.-Eur. J.*, 2010, **16**, 4368–4380.
- 45 V. Amendola, L. Fabbri, L. Mosca and F. P. Schmidtchen, *Chem.-Eur. J.*, 2011, **17**, 5972–5981.



- 46 A. Rostami, C. J. Wei, G. Guérin and M. S. Taylor, *Angew. Chem.*, 2011, **123**, 2107–2110.
- 47 N. Busschaert, I. L. Kirby, S. Young, S. J. Coles, P. N. Horton, M. E. Light and P. A. Gale, *Angew. Chem.*, 2012, **124**, 4502–4506.
- 48 N. Busschaert, R. B. P. Elmes, D. D. Czech, X. Wu, I. L. Kirby, E. M. Peck, K. D. Hendzel, S. K. Shaw, B. Chan, B. D. Smith, K. A. Jolliffe and P. A. Gale, *Chem. Sci.*, 2014, **5**, 3617.
- 49 A. Aydogan, D. J. Coady, V. M. Lynch, A. Akar, M. Marquez, C. W. Bielawski and J. L. Sessler, *Chem. Commun.*, 2008, **12**, 1455–1457.
- 50 P. Sokkalingam, S. J. Hong, A. Aydogan, J. L. Sessler and C. H. Lee, *Chem.–Eur. J.*, 2013, **19**, 5860–5867.
- 51 A. Aydogan and A. Akar, *Chem.–Eur. J.*, 2012, **18**, 1999–2005.
- 52 A. Aydogan, D. J. Coady, S. K. Kim, A. Akar, C. W. Bielawski, M. Marquez and J. L. Sessler, *Angew. Chem., Int. Ed.*, 2008, **47**, 9648–9652.
- 53 H. Kim, K. I. Hong, J. H. Lee, P. Kang, M. G. Choi and W. D. Jang, *Chem. Commun.*, 2018, **54**, 10863–10865.
- 54 K. P. McDonald, B. Qiao, E. B. Twum, S. Lee, P. J. Gamache, C. H. Chen, Y. Yi and A. H. Flood, *Chem. Commun.*, 2014, **50**, 13285–13288.
- 55 P. Bose, R. Dutta, S. Santra, B. Chowdhury and P. Ghosh, *Eur. J. Inorg. Chem.*, 2012, **35**, 5791–5801.
- 56 W. Liu, A. G. Oliver and B. D. Smith, *J. Org. Chem.*, 2019, **84**, 4050–4057.
- 57 L. H. Bowen and T. R. Rood, *J. Inorg. Nucl. Chem.*, 1966, **28**, 1985–1990.
- 58 V. K. Davis, C. M. Bates, K. Omichi, B. M. Savoie, N. Momcilovic, Q. Xu, W. J. Wolf, M. A. Webb, K. J. Billings, N. H. Chou, S. Alayoglu, R. Mckenney, I. M. Darolles, N. G. Nair, A. Hightower, D. Rosenberg, M. Ahmed, C. J. Brooks, T. F. Miller III, R. H. Grubbs and S. C. Jones, *Science*, 2018, **362**, 1144–1148.
- 59 P. R. Wittbrodt and C. D. Palmer, *Environ. Sci. Technol.*, 1995, **29**, 255–263.
- 60 I. Ravikumar and P. Ghosh, *Chem. Soc. Rev.*, 2012, **41**, 3077–3098.
- 61 B. A. Moyer, R. Custelcean, B. P. Hay, J. L. Sessler, K. Bowman-James, V. W. Day and S. O. Kang, *Inorg. Chem.*, 2013, **52**, 3473–3490.
- 62 S. Q. Chen, W. Zhao and B. Wu, *Front. Chem.*, 2022, **10**, 905563.
- 63 H. Kaur, S. Sinha, V. Krishnan and R. R. Koner, *Dalton Trans.*, 2021, **50**, 8273–8291.
- 64 M. D. Cohen, B. Kargacin, C. B. Klein and M. Costa, *Crit. Rev. Toxicol.*, 1993, **23**, 255–281.
- 65 M. Bayrakci and Ş. Yiğiter, *Tetrahedron*, 2013, **69**, 3218–3224.
- 66 S. Sayin, S. Eymur and M. Yilmaz, *Ind. Eng. Chem. Res.*, 2014, **53**, 2396–2402.
- 67 C. A. Seipp, N. J. Williams, V. S. Bryantsev and B. A. Moyer, *Sep. Sci. Technol.*, 2018, **53**, 1864–1873.
- 68 N. J. Williams, C. A. Seipp, K. A. Garrabrant, R. Custelcean, E. Holguin, J. K. Keum, R. J. Ellis and B. A. Moyer, *Chem. Commun.*, 2018, **54**, 10048–10051.
- 69 D. J. Wood and J. D. Law, *Sep. Sci. Technol.*, 1997, **32**, 241–253.
- 70 M. L. Dietz, E. P. Horwitz and R. D. Rogers, *Solvent Extr. Ion Exch.*, 1995, **13**, 1–17.
- 71 K. Gloe, H. Stephan and M. Grotjahn, *Chem. Eng. Technol.*, 2003, **26**, 1107–1117.
- 72 C. J. Borman, R. Custelcean, B. P. Hay, N. L. Bill, J. L. Sessler and B. A. Moyer, *Chem. Commun.*, 2011, **47**, 7611–7613.
- 73 L. R. Eller, M. Stępień, C. J. Fowler, J. T. Lee, J. L. Sessler and B. A. Moyer, *J. Am. Chem. Soc.*, 2007, **129**, 11020–11021.
- 74 C. J. Fowler, T. J. Haverlock, B. A. Moyer, J. A. Shriver, D. E. Gross, M. Marquez, J. L. Sessler, A. Hossain and K. Bowman-James, *J. Am. Chem. Soc.*, 2008, **130**, 14386–14387.
- 75 C. J. Borman, R. Custelcean, B. P. Hay, N. L. Bill, J. L. Sessler and B. A. Moyer, *Chem. Commun.*, 2011, **47**, 7611–7613.
- 76 B. A. Moyer, F. V. Sloop Jr, C. J. Fowler, T. J. Haverlock, H. A. Kang, L. H. Delmau, D. M. Bau, M. A. Hossain, K. Bowman-James, J. A. Shriver, N. L. Bill, D. E. Gross, M. Marquez, V. M. Lynch and J. L. Sessler, *Supramol. Chem.*, 2010, **22**, 653–671.
- 77 S. K. Kim, J. Lee, N. J. Williams, V. M. Lynch, B. P. Hay, B. A. Moyer and J. L. Sessler, *J. Am. Chem. Soc.*, 2014, **136**, 15079–15085.
- 78 R. Custelan, *Chem. Commun.*, 2013, **49**, 2173–2182.
- 79 C. Jia, B. Wu, S. Li, X. Huang, Q. Zhao, Q.-S. Li and X.-J. Yang, *Angew. Chem., Int. Ed.*, 2011, **50**, 486–490.
- 80 S. Q. Chen, S. N. Yu, W. Zhao, L. Liang, Y. Gong, L. Yuan, J. Tang, X. J. Yang and B. Wu, *Inorg. Chem. Front.*, 2022, **9**, 6091–6101.
- 81 B. Akhuli, I. Ravikumar and P. Ghosh, *Chem. Sci.*, 2012, **3**, 1522–1530.
- 82 R. Dutta, S. Chakraborty, P. Bose and P. Ghosh, *Eur. J. Inorg. Chem.*, 2014, **25**, 4134–4143.
- 83 L. Qin, S. J. N. Vervuurt, R. B. P. Elmes, S. N. Berry, N. Proschogo and K. A. Jolliffe, *Chem. Sci.*, 2020, **11**, 201–207.
- 84 S. K. Dey, S. Pereira, S. S. Harmalkar, S. N. Mhaldar, V. V. Gobrea and C. Janiak, *CrystEngComm*, 2020, **22**, 6152–6160.
- 85 S. K. Dey, B. G. Hernández, V. V. Gobre, D. Woschko, S. S. Harmalkar, F. R. Gayen, B. Saha, R. L. Goswamee and C. Janiak, *Dalton Trans.*, 2022, **51**, 15239.
- 86 R. Alberto, G. Bergamaschi, H. Braband, T. Fox and V. Amendola, *Angew. Chem.*, 2012, **124**, 9910–9914.
- 87 V. Amendola, G. Alberti, G. Bergamaschi, R. Biesuz, M. Boiocchi, S. Ferrito and F.-P. Schmidtchen, *Eur. J. Inorg. Chem.*, 2012, **21**, 3410–3417.
- 88 G. V. Kolesnikov, K. E. German, G. Kirakosyan, I. G. Tananaev, Y. A. Ustynyuk, V. N. Khrustalev and E. A. Katayev, *Org. Biomol. Chem.*, 2011, **9**, 7358–7364.
- 89 W. Zhou, A. Li, P. A. Gale and Q. He, *Cell Rep.*, 2022, **3**, 100875.
- 90 D. Zhang, T. K. Ronson, J. Mosquera, A. Martinez and J. R. Nitschke, *Angew. Chem., Int. Ed.*, 2018, **57**, 3717–3721.
- 91 H. Zeng, P. Liu, G. Feng and F. Huang, *J. Am. Chem. Soc.*, 2019, **141**, 16501–16511.





- 92 T. K. Ghosh, S. Chakraborty, B. Chowdhury and P. Ghosh, *Inorg. Chem.*, 2017, **56**, 5371–5382.
- 93 R. Andrews, S. Begum, C. J. Clemett, R. A. Faulkner, M. L. Ginger, J. Harmer, M. Molinari, G. M. B. Parkes, Z. M. H. Qureshi, C. R. Rice, M. D. Ward, H. M. Williams and P. B. Wilson, *Angew. Chem., Int. Ed.*, 2020, **132**, 20660–20664.
- 94 S. Dubchak, *Impact of Caesium on Plants and the Environment*, ed. D. K. Gupta and C. Walther, Springer International Publishing, Cham, 2017; pp. pp. 1–18.
- 95 G. U. Akkuş and S. Aslan, *Int. J. Org. Chem.*, 2017, **7**, 301–311.
- 96 R. Yi, C. Xu, T. Sun, Y. Wang, G. Ye, S. Wang and J. Chen, *Sep. Purif. Technol.*, 2018, **199**, 97–104.
- 97 L. Gupta, A. C. Hoepker, K. J. Singh and D. B. Collum, *J. Org. Chem.*, 2009, **74**, 2231–2233.
- 98 H. Haferkamp, M. Niemeyer, R. Boehm, U. Holzkamp, C. Jaschik and V. Kaese, *Mater. Sci. Forum*, 2000, **350**, 31–42.
- 99 C. Grosjean, P. Herrera Miranda, M. Perrin and P. Poggi, *Renewable Sustainable Energy Rev.*, 2012, **16**, 1735–1744.
- 100 O. A. Avramchik, E. I. Korotkova, E. V. Plotnikov, A. N. Lukina and Y. A. Karbainov, *J. Pharm. Biomed. Anal.*, 2005, **37**, 1149–1154.
- 101 I. Oral and V. Abetz, *Macromol. Rapid Commun.*, 2021, **42**, 2000746.
- 102 C. J. Pedersen, *J. Am. Chem. Soc.*, 1967, **89**, 7017–7036.
- 103 C. J. Pederson, *J. Am. Chem. Soc.*, 1967, **89**, 2495–2496.
- 104 I. Oral and V. Abetz, *Soft Matter*, 2022, **18**, 934–937.
- 105 J. Zhang, M. Wenzel, J. Steup, G. Schaper, F. Hennersdorf, H. Du, S. Zheng, L. F. Lindoy and J. J. Weigand, *Chem.–Eur. J.*, 2022, **28**, e2021036.
- 106 M. T. Reetz, C. M. Niemeyer and K. Harms, *Angew. Chem., Int. Ed.*, 1991, **30**, 1472–1474.
- 107 A. J. McConnell and P. D. Beer, *Angew. Chem., Int. Ed.*, 2012, **51**, 5052–5061.
- 108 A. McConnell, A. Docker and P. Beer, *ChemPlusChem*, 2020, **85**, 1824–1841.
- 109 S. A. Wagay, L. Khan and R. Ali, *Chem.–Asian J.*, 2022, e202201080.
- 110 Q. He, N. J. Williams, J. H. Oh, V. M. Lynch, S. K. Kim, B. A. Moyer and J. L. Sessler, *Angew. Chem., Int. Ed.*, 2018, **57**, 11924–11928.
- 111 K. I. Hong, H. Kim, Y. Kim, M. G. Choi and W.-D. Jang, *Chem. Commun.*, 2020, **56**, 10541–10544.
- 112 D. Jaglenieć, S. Siennicka, Ł. Dobrzycki, M. Karbarz and J. Romański, *Inorg. Chem.*, 2018, **57**, 12941–12952.
- 113 K. Maršálek and V. Šindelář, *Org. Lett.*, 2020, **22**, 1633–1637.
- 114 N. A. D. Simone, M. Chvojka, J. Lapešová, L. Martínez-Crespo, P. Slávik, J. Sokolov, S. J. Butler, H. Valkenier and V. Šindelář, *J. Org. Chem.*, 2022, **87**, 9829–9838.
- 115 I. Ravikumar, S. Saha and P. Ghosh, *Chem. Commun.*, 2011, **47**, 4721–4723.
- 116 S. K. Kim, V. M. Lynch, N. J. Young, B. P. Hay, C.-H. Lee, J. S. Kim, B. A. Moyer and J. L. Sessler, *J. Am. Chem. Soc.*, 2012, **134**, 20837–20843.
- 117 M. Zakrzewski, D. Załubiniak and P. Piątek, *Dalton Trans.*, 2018, **47**, 323–330.
- 118 C. Wang, Z. Wang and X. Zhang, *Acc. Chem. Res.*, 2012, **45**, 608–618.
- 119 X. Chi, G. M. Peters, F. Hammel, C. Brockman and J. L. Sessler, *J. Am. Chem. Soc.*, 2017, **139**, 9124–9127.
- 120 X. Chi, G. M. Peters, C. Brockman, V. M. Lynch and J. L. Sessler, *J. Am. Chem. Soc.*, 2018, **140**, 13219–13222.
- 121 Q. He, Z. Zhang, J. T. Brewster, V. M. Lynch, S. K. Kim and J. L. Sessler, *J. Am. Chem. Soc.*, 2016, **138**, 9779–9782.
- 122 Q. He, G. M. Peters, V. M. Lynch and J. L. Sessler, *Angew. Chem., Int. Ed.*, 2017, **56**, 13396–13400.
- 123 B. M. Rambo, S. K. Kim, J. S. Kim, C. W. Bielawski and J. L. Sessler, *Chem. Sci.*, 2010, **1**, 716–722.
- 124 Y. Yeon, S. Leem, C. Wagen, V. M. Lynch, S. K. Kim and J. L. Sessler, *Org. Lett.*, 2016, **18**, 4396–4399.
- 125 S. K. Kim, G. I. Vargas-Zúñiga, B. P. Hay, N. J. Young, L. H. Delmau, C. Masselin, C.-H. Lee, J. S. Kim, V. M. Lynch, B. A. Moyer and J. L. Sessler, *J. Am. Chem. Soc.*, 2012, **134**, 1782–1792.
- 126 J. Romański and P. Piątek, *Chem. Commun.*, 2012, **48**, 11346–11348.
- 127 P. Piątek, M. Karbarz and J. Romański, *Dalton Trans.*, 2014, **43**, 8515–8522.
- 128 M. Zakrzewski, N. Kwietniewska, W. Walczaka and P. Piątek, *Chem. Commun.*, 2018, **54**, 7018–7021.
- 129 M. Zakrzewski and P. Piątek, *New J. Chem.*, 2021, **45**, 18635–18640.
- 130 D. Jaglenieć, Ł. Dobrzycki, M. Karbarz and J. Romański, *Chem. Sci.*, 2019, **10**, 9542–9547.
- 131 M. Zaleskaya, M. Karbarz, M. Wilczek, Ł. Dobrzycki and J. Romański, *Inorg. Chem.*, 2020, **59**, 13749–13759.

